

Disclaimer: This is a pre-publication version. Readers are recommended to consult the full published version for accuracy and citation. Published in *Analytica Chimica Acta*, 912, 32-40 (2016). doi.org/10.1016/j.aca.2016.01.035.

## **Absence of Gradients and Nernstian Equilibrium Stripping (AGNES) for the determination of [Zn<sup>2+</sup>] in estuarine waters**

Holly Pearson<sup>1</sup>, Josep Galceran<sup>2</sup>, Encarna Companys<sup>2</sup>, Charlotte Braungardt<sup>1</sup>, Paul Worsfold<sup>1</sup>, Jaume Puy<sup>2</sup>, Sean Comber<sup>1\*</sup>

<sup>1</sup> Biogeochemistry Research Centre, Plymouth University, Drake Circus, Plymouth PL4 8AA, UK.

<sup>2</sup> University of Lleida, Departament de Química, UdL and Agrotecnio. Av. Rovira Roure 191, 25198 Lleida, SPAIN.

\* Corresponding Author: [sean.comber@plymouth.ac.uk](mailto:sean.comber@plymouth.ac.uk)

**Key words:** zinc, free ion, AGNES, estuarine water, environmental quality standards, voltammetry.

### **Highlights:**

- AGNES allows direct determination of free Zn<sup>2+</sup> ion
- First application of AGNES to estuarine waters
- Results can be used for toxicity modelling and setting appropriate Environmental Quality Standards (EQS)
- Good agreement with competitive ligand exchange cathodic stripping voltammetry

### **Abstract**

Zinc (Zn) has been classified as a “Specific Pollutant” under Annex VIII of the EU Water Framework Directive by two thirds of the EU member states. As a result, the

UK Environmental Quality Standard (EQS) for Transitional and Coastal (TrAC) Waters has been reduced from 612 nM to 121 nM total dissolved Zn. It is widely accepted that the free metal ion ( $[Zn^{2+}]$ ) is the most bioavailable fraction, but there are few techniques available to determine its concentration in these waters. In this work, Absence of Gradients and Nernstian Equilibrium Stripping (AGNES) has been applied, for the first time, to determine  $[Zn^{2+}]$  in estuarine waters. The AGNES method had a mean RSD of  $\pm 18\%$ , a (deposition time dependent) limit of detection of 0.73 nM and a  $[Zn^{2+}]$  recovery of  $112 \pm 19\%$  from a certified reference material (BCR-505; Estuarine Water). AGNES results for 13 estuarine samples (salinity 0.1 – 31.9) compared well ( $P = 0.02$ ) with Competitive Ligand Exchange Cathodic Stripping Voltammetry (CLE-AdCSV) except for one sample. AGNES requires minimal sample manipulation, is unaffected by adsorption of interfering species at the electrode surface and allows direct determination of free zinc ion concentrations. Therefore AGNES results can be used in conjunction with ecotoxicological studies and speciation modelling to set and test compliance with water quality standards.

## 1. Introduction

Zinc (Zn) is an essential trace element and plays an important role in certain DNA binding proteins and hydrolytic enzymes [1], but uptake by biota in excess of required concentrations can result in toxic effects. The free metal ion is recognised as the most readily bioavailable species and, therefore, is of greatest concern with respect to permeation through biological membranes and potential toxicity [2].

The new UK Environmental Quality Standard (EQS) for Zn in saltwater is 121 nM, which includes a natural background concentration of 17 nM, and is significantly lower than the previous EQS of 612 nM. Unlike the Zn EQS set for freshwaters, the saltwater EQS refers to total dissolved Zn and does not account of the bioavailability of different Zn species [3]. Recently Stockdale et al. [4] highlighted the relative lack of data published on  $[Zn^{2+}]$  in saline waters compared with other metals such as Cu. Copper in estuarine waters is strongly complexed by humic and fulvic acids (> 90 %) and reported  $[Cu^{2+}]$  are frequently of the order  $10^{-13} - 10^{-11}$  M [5-7], but can be as low as  $10^{-15}$  M [5]. In contrast, reported  $[Zn^{2+}]$  are typically of the order  $10^{-9}$  M [8-11], with

24 – 98 % organically complexed, suggesting a weaker affinity for binding by organic ligands [12]. Only four studies report  $[Zn^{2+}]$  in estuarine waters over a wide salinity range (Table 1). This lack of data is due in part to the analytical challenges associated with determining ultra-trace  $[Zn^{2+}]$  concentrations (pM - nM) in complex environmental matrices. Free  $Zn^{2+}$  concentrations are therefore more often predicted than measured. Various codes (e.g. the Windermere Humic Aqueous Model (WHAM) [13] and Visual Minteq (VMINTEQ) [14]) have been developed to predict free metal ion concentrations ( $[Me^{n+}]$ ) in freshwaters based on total dissolved concentrations and ambient water quality parameters (e.g. pH, hardness, dissolved organic carbon, etc.). The calculated  $[Me^{n+}]$  have been combined with ecotoxicological data to generate site specific freshwater quality standards for metals such as Cu, Ni and Zn, using the Biotic Ligand Model [15, 16]. However, the lack of data on Zn speciation in estuaries has constrained the derivation of a robust Zn EQS for TrAC Waters.

**Table 1** Free zinc ion concentrations in estuarine waters reported in the literature. DPASV: differential pulse anodic stripping voltammetry, CLE-AdCSV: competitive ligand exchange adsorptive cathodic stripping voltammetry.

Location	Salinity range	$[Zn^{2+}]$ range (nM)	Analytical Technique	Reference
Narragansett Bay Rhode Island, USA	24 – 30	0.3 – 13	DPASV	[9]
Cape Fear Estuary North Carolina, USA	7 – 32	0.13 – 16	CLE-AdCSV	[8]
Scheldt Estuary, SW Netherlands	9 – 27	2 – 16	CLE-AdCSV	[17]
Gulf of Thailand, SE Asia	1.8 - 31.2	0.63 – 39.3	MnO <sub>2</sub> equilibration	[18]

Voltammetric techniques can be used to study Zn speciation in estuarine waters, e.g. competitive ligand exchange adsorptive cathodic stripping voltammetry (CLE-AdCSV) [19] and anodic stripping voltammetry (ASV) [20]. With these techniques,  $[Zn^{2+}]$  is calculated from measured total and labile Zn concentrations, while ligand

concentrations and conditional stability constants between Zn and (organic) ligands in the sample can be determined within operationally defined detection windows after titration of subsamples spiked with Zn [21]. Limitations of this approach include (i) the analysis of titration data requires assumptions about Zn-ligand complexation characteristics (e.g. 1:1 binding [22]), (ii) sample preparation requires lengthy equilibration (> 15 h) and (iii) a single titration requires at least 150 mL of sample. Consequently, replicate titrations are limited and precision data are rarely reported.

Absence of Gradients and Nernstian Equilibrium Stripping (AGNES) is an electrochemical stripping technique designed for the direct determination of free Zn ion concentrations in solution [23]. The analytical procedure consists of two stages, (i) application of a suitable potential to preconcentrate the determinand within the working electrode (a mercury drop or thin layer) by a known factor (the “gain”  $Y$ ) for a deposition time long enough to achieve equilibrium of the metal species within the bulk solution, within the working electrode, and between them [24], and (ii) electrochemical stripping of the  $Zn^0$  from the electrode, where the response function (current or charge) of AGNES is proportional to the free Zn ion concentration in the solution [25, 26].

With a hanging mercury drop electrode (HMDE), the technique has been used to determine  $[Zn^{2+}]$  in seawater [11], extracts of dissolved organic matter from treated wastewater [27], freshwater [28], soil extracts [29], nanoparticle dispersions [30, 31], and wine [32]. Results obtained using AGNES have been compared with data from the Donnan membrane technique [29], resin titrations [33], ion-selective electrodes [23, 34], and scanned stripping chronopotentiometry [35, 36]. There are no reported data, however, for TrAC Waters with widely varying ionic strength, which is critical for setting suitable EQSs and subsequent compliance monitoring.

The overall aim of this work was to demonstrate the suitability of the AGNES technique for determining  $[Zn^{2+}]$  in TrAC Waters by i) optimising AGNES for estuarine samples (salinities 0.1 – 31.9), ii) determining the analytical figures of merit for the optimised method and iii) comparing the performance characteristics of AGNES with CLE-AdCSV in samples collected in three different seasons from the temperate, macro-tidal Tamar Estuary (SW England).

## 2. Experimental

### 2.1 Reagents

Ultra-high purity (UHP) water (Elga Process Water, resistivity = 18.2 MΩ cm) was used for all applications. All bottles for Zn (low density polyethylene LDPE, Nalgene, 500 mL), and for DOC (Pyrex glass, Fisher Scientific), filtration equipment for Zn (polysulphone, Nalgene) and DOC (Glass, Millipore), and vials (glass, VWR) were cleaned in dilute HCl (10% HCl, Fisher Scientific) and rinsed with UHP water. Filter membranes used for Zn determination (0.2 and 0.4 μm Whatman, Nuclepore polycarbonate track-etched) were soaked overnight in dilute (25 %) HCl and oven heated to 60 °C [37], before copious rinsing with UHP water. Because the 0.4 μm polycarbonate filters cannot be ashed, the accepted method for DOC determination was used, employing glass fibre membranes [38] (GF/F, 0.7 μm, Whatman, Fisher Scientific). Glass vials, filter equipment and membranes were ashed for 6 h at 550 °C prior to use.

Aqueous calibration standards containing 1 μM, 15.3 μM and 1.53 mM Zn were prepared by dilution of Zn nitrate element reference solution (15.3 mM PrimAg, ROMIL) with UHP water and acidified to pH 2 (HCl, ROMIL). Synthetic calibration solutions of appropriate ionic strength were made up using potassium nitrate (TraceSelect, Sigma Aldrich) and UHP water.

4-(2-hydroxyethyl)-1-piperazineethanesulfonic acid (HEPES, high purity, VWR) buffer (1 M) was prepared from solids in UHP water and adjusted with ammonium hydroxide solution (SpA, ROMIL) to hold samples at pH 7.8. Ammonium pyrrolidine dithiocarbamate (APDC, Fisher Scientific) stock solution (0.1 M) was prepared from solids in UHP water. This concentration was used for the “two point method” (TPM, section 2.3.2) using 250 μM APDC. APDC stock was diluted (to 0.01 M) for titrations with 40 μM APDC. Hydrogen peroxide (Suprapur, Merck) was added to samples during UV irradiation prior to analysis of total dissolved Zn (TDZn).

The complete certificate of analysis for the certified reference material used to assess the accuracy of each technique (estuarine water “BCR 505”) gives consensus values in nmol/kg for the total metal concentrations of four metals: Cd

$0.80 \pm 0.04$  (n = 12), Cu  $29.4 \pm 1.5$  (n = 12), Ni  $24.1 \pm 2.0$  (n = 10), and Zn  $172 \pm 11$  (n= 15).

## *2.2 Sample collection, treatment and storage*

Thirteen samples were collected during three surveys (spring and summer 2014 and winter 2015) across the full range of estuarine salinities, from the fresh water end member of the Tamar River to the mouth of its estuary in the English Channel (SW England). A map of sampling sites is given in Fig. S1.

Samples were collected using a sampling device [39] that carried six sampling bottles (500 mL LDPE bottles for metal, and 500 mL glass for DOC) and was triggered at 1 m below the surface by a messenger. Samples for Zn determination were filtered within 48 h of collection, first to 0.4  $\mu\text{m}$ , then a sub-sample additionally to 0.2  $\mu\text{m}$ , in order to assess any variation in the association of Zn with colloidal material. Filtration units were rinsed with ca. 150 mL UHP water between each sample and, following assemblage with the membrane, were rinsed with UHP water and sample. Filtered sample was poured into preconditioned (rinsed with filtrate) bottles and kept refrigerated at 4 °C. Procedural blanks for Zn were stored in clean LDPE bottles and acidified (6 M HCl, SpA, ROMIL) to ca. pH 2. Samples for DOC were collected in glass bottles, filtered on-site, acidified to ca. pH 2 (6 M HCl, SpA, ROMIL) and stored in glass vials prior to analysis.

In situ pH was measured using a calibrated pH meter (model H19025, Hanna Instruments Ltd., UK) and salinity was determined in un-filtered samples using a calibrated salinometer (Orion model 105).

Samples for total and labile Zn determination by CLE-AdCSV were refrigerated (4 °C) immediately after collection and analysed within 48 h. Samples for the determination of Zn complexation capacity and  $[\text{Zn}^{2+}]$  were stored at -18 °C.

### 2.3 Instrumentation and Procedures

For both methods, samples were analysed within 48 h of being slowly thawed at 4 °C. Sample preparation was undertaken in a class 100 laminar flow unit. Clean borosilicate glass voltammetric cells were used for calibration (AGNES) and sample analysis. A complete description of the methods is provided in the electronic supporting information (ESI) sections 2 and 3.

#### 2.3.1 AGNES optimisation for estuarine waters

For AGNES a HMDE set at drop size 1 (radius  $1.41 \times 10^{-4}$  m  $\pm$  10 %, Metrohm) was used on a VA 663 stand (Metrohm), which was connected to a  $\mu$ Autolab voltammeter (EcoChemie) via an interface (IME, EcoChemie). The Ag/AgCl reference electrode (Metrohm) was filled with electrolyte solution (3 M KCl) containing AgCl (Thermo Orion, cat. code 900011) and the electrolyte bridge contained 0.1 M KNO<sub>3</sub> (Trace Select, Sigma Aldrich). The software used for peak analysis was GPES version 4.9.

The ionic strength ( $\mu$ ) of individual estuarine samples during analysis was calculated using an ion pairing model [40] with metal complexation constants from Turner et al. [41] combined with inputs of salinity and pH. CO<sub>2</sub> was omitted as it was removed during sample purge with ultrapure N<sub>2</sub> prior to analysis. Five synthetic calibration solutions (A – E, Table 2) of KNO<sub>3</sub> were prepared to represent the mean ionic strengths of groups of samples of similar salinities. Calibration was carried out in each of the KNO<sub>3</sub> solutions and in a separate cell to that of the samples to minimise the risk of cross contamination. Calibration can be performed at high concentrations with a low gain (and short deposition periods) to save time [23]. This is possible because of the proportionality between the applied gain and the faradaic current obtained during stripping (equations 2 and 3). The analytical responses in the calibration were sought to fall in the range of current (or charge) responses expected for the samples, because they corresponded to similar values of the product  $Y$  times  $[\text{Zn}^{2+}]$  (i.e. this product is just  $[\text{Zn}^0]$  according to the Nernst equation used in AGNES) (Fig. 1).

In this study, calibration was undertaken with an AGNES 1P programme where  $Y = 5$  during deposition ( $t_1 = 50$  s). During stripping (calibration, blanks and all samples) a potential ( $E_2$ ) corresponding to  $Y = 10^{-8}$  was applied for a fixed time ( $t_2 = 50$  s) (ESI section 1.1). The current was measured every 0.05 s during stripping and the analytical response for current was taken after 0.2 s (this time gave the maximum signal:noise ratio [23]). The current (or charge) values at the tail of the stripping curve were used to correct for residual dissolved oxygen (see below). At each ionic strength, four standard additions were made in each AGNES calibration.

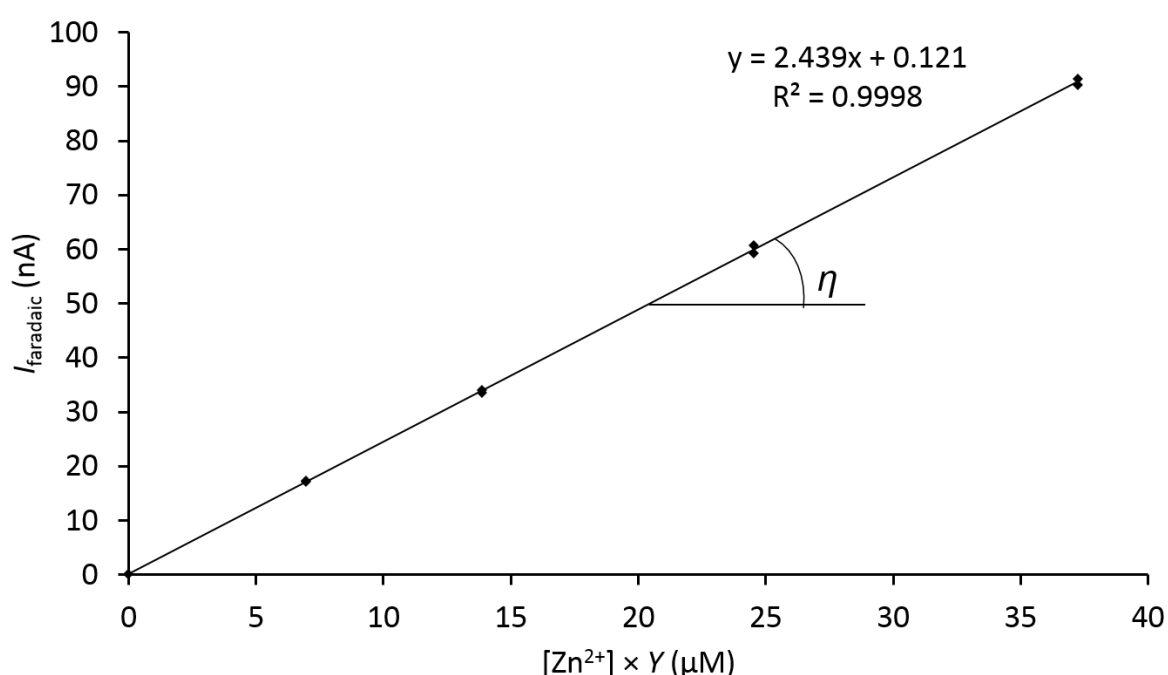


**Fig. 1** An example calibration plot (determined using an AGNES single potential programme ( $[\text{KNO}_3] = 0.393$  M,  $Y = 4.44$ ).  $\text{Eta } (\eta) = 2.439 \times 10^{-3} \text{ A M}^{-1}$  is obtained from the slope and  $I_{\text{faradaic}}$  is the current value obtained from stripping minus the shifted blank. Data points represent duplicate AGNES analyses performed on each zinc addition. This kind of representation highlights the possibility of using different gains for calibrations and sample analyses.

During calibration, the peak potential for Zn ( $E_{\text{peak}}$ ) at different ionic strengths was determined with a differential pulse polarography (DPP) experiment (modulation time 0.05 s, interval time 1 s, initial potential -0.82 V, final potential -1.02 V, step potential 1.05 mV, modulation amplitude 49.95 mV) [23]. The  $E_{\text{peak}}$  was used to calculate the deposition potential ( $E_1$ ), which is related to the gain through the Nernst equation



(ESI section 2.4). Because  $E_{\text{peak}}$  changes with ionic strength, due to the differences in the metal activity coefficient  $\gamma_{\text{M}}$  [42], potentials were determined based on an average ionic strength from grouped samples with a further fine-tuning correction (Table 2). The actual  $Y$  value applied to a sample of a given grouping of ionic strengths was calculated from the associated calibration using:

$$Y = \frac{\frac{\gamma_{\text{Zn}}}{\gamma_{\text{Zn}}^{\mu_{\text{calib}}}} \sqrt{\frac{D_{\text{Zn}}}{D_{\text{Zn}}^0}}}{\exp\left[\left(E_1 - E_{\text{peak}}^{\mu_{\text{calib}}} - \frac{\Delta E}{2}\right) \frac{nF}{RT}\right]} \quad (1)$$

Where  $E_{\text{peak}}^{\mu_{\text{calib}}}$  is the peak potential obtained from a DPP experiment in the corresponding calibration solution (one of A - E),  $D_{\text{Zn}}$  and  $D_{\text{Zn}}^0$  are the diffusion coefficients for oxidized and reduced Zn respectively, and  $\Delta E$  is the modulation amplitude of the DPP experiment (in V).

For samples with ionic strengths  $<0.1$  M, the charge was used instead of the current to quantify  $[\text{Zn}^{2+}]$  to avoid any anomalous stripping behaviour affecting low ionic strength media [42].

The slope of calibration plots of the faradaic current ( $I_f$ ) (or the charge,  $Q$ ) vs.  $Y_{\text{calibration}} \times [\text{Zn}^{2+}]$  (Fig. 1) corresponds to the proportionality factor eta ( $\eta$ , or  $\eta_Q$  when charge is used). This was used to calculate  $[\text{Zn}^{2+}]$  in the sample as follows:

$$[\text{Zn}^{2+}] = \frac{I_f}{(Y\eta)} \quad (2)$$

and for low ionic strength samples:

$$[\text{Zn}^{2+}] = \frac{Q}{(Y\eta_Q)} \quad (3)$$

The range of eta values obtained in this work compares well with the values obtained by other workers using AGNES calibrated at  $\mu \leq 0.1$  M ( $2.1 \times 10^{-3}$  amps per molar ( $\text{A M}^{-1}$ ) [43],  $2.4 \times 10^{-3}$   $\text{A M}^{-1}$  [44]), at  $\mu = 0.5$  M ( $2.08 \times 10^{-3}$   $\text{A M}^{-1}$  [11]) and  $\mu = 0.7$  M ( $3.06 \times 10^{-3}$   $\text{A M}^{-1}$  [11]).

The expected  $[\text{Zn}^{2+}]$  in the calibrations were calculated using the speciation computer code Visual MINTEQ (VMINTEQ) version 3.1 [14]. The activity coefficient was calculated using  $\{\text{Zn}^{2+}\} / [\text{Zn}^{2+}]$  from VMINTEQ which relies on Davies equation. As an example, input parameters used for solution D are given in ESI section 2.5.

For the estuarine samples,  $[Zn^{2+}]$  was analysed in 10 mL aliquots using the 2P AGNES programme (ESI section 2.2). Although not strictly required, for the sake of matrix matching, the HEPES buffer used for CLE-AdCSV was also added to the samples for the AGNES procedure. Due to the low concentration of free Zn, a large gain is required, which would impose prohibitively long times with the simplest 1P deposition program. A faster variant consists in the splitting of the stirring period of the deposition stage into two sub-stages: one, for  $t_{1,a}$  seconds, under diffusion limited conditions, and another one, for  $t_{1,b}$  seconds, at the desired gain [45]. As a check for consistency, two different gains and three deposition times ( $t_{1,a}$  and  $t_{1,b}$ ) for each gain setting were used following the general rule  $t_{1,a} = 0.7 \times Y$  and  $t_{1,b} = 3 \times t_{1,a}$ . The  $[Zn^{2+}]$  in each sample was calculated using the stripping current (or charge) obtained after application of the longest deposition time [43]. Two repeat AGNES analyses were conducted on each sample aliquot, at each deposition time, for both gains (therefore  $n = 4$ ).

**Table 2** Synthetic calibration solutions for AGNES, matching ionic strength of estuarine samples (July & April 2014, February 2015). IS: intermediate salinity, SW: sea water end member, FW fresh water end member, numbers refer to distance (in km) from Gunnislake Weir, <sup>a</sup>0.2  $\mu m$  filter fraction, <sup>b</sup>0.4  $\mu m$  filter fraction,  $\mu$ : the ionic strength of the solution,  $\eta$  and  $\eta_Q$ : eta and eta-Q, the proportionality factor obtained from an AGNES calibration plot using current or charge as the response function, respectively (see text and ESI section 2.5),  $AM^{-1}$ : amps per molar,  $Y_{calibration}$ : gain used for analysis of calibration solutions. For salinities < 0.5, the charge Q was used (highlighted in bold) to compute  $[Zn^{2+}]$ .

<b>Solution</b>	<b>Salinity</b>	<b><math>\mu</math> <math>KNO_3</math> (mol L<sup>-1</sup>)</b>	<b>Samples calibrated</b>	<b><math>Y_{calibration}</math></b>	<b><math>\eta</math> (AM<sup>-1</sup>) or <math>\eta_Q</math> (C M<sup>-1</sup>)</b>
A	< 0.5	0.007	FW-1.1 <sup>a</sup> , FW-1.1 <sup>b</sup> (summer & winter), IS4.8 <sup>b</sup>	<b>4.03</b>	<b>0.0018</b>
B	3 – 10	0.195	IS13.3 <sup>b</sup> , IS14 <sup>b</sup> , IS19.5 <sup>b</sup>	4.93	0.0022
C	10 – 20	0.291	IS24 <sup>b</sup> , IS19.5 <sup>b</sup>	5.27	0.0022
D	20 – 30	0.393	IS25 <sup>b</sup> , SW32 <sup>b</sup> (winter)	4.44	0.0024
E	> 30	0.688	SW32 <sup>a</sup> , SW32 <sup>b</sup> (spring)	5.11	0.0028

### 2.3.1.1 AGNES analytical figures of merit

The accuracy of AGNES was assessed by analysing an estuarine water CRM of salinity 12.1 (CRM BCR-505, European Commission; [46]) with a certified value of  $172 \pm 11 \text{ nmol kg}^{-1}$  TDZn. The CRM was analysed at pH 1.5 following calibration in  $\text{KNO}_3$  at the same pH and ionic strength (0.228 M) as BCR-505.

To determine the non-faradaic (capacitive) contribution to the AGNES response, an AGNES analysis was performed on a sample with a shift in the deposition and stripping potentials ( $E_{1,\text{sb}}$  and  $E_{2,\text{sb}}$ , respectively), at a potential at which there was a negligible accumulation of Zn. This is termed a “shifted blank” (Fig. S6) [11]. In order to determine the necessary shifted blank deposition time ( $t_{1,\text{sb}}$ ), an intermediate salinity estuarine sample was analysed using an  $E_{1,\text{sb}}$  with increasing deposition time  $t_{1,\text{sb}}$  (50 – 1000 s), whereby 50 s was identified as optimum (ESI section 2.3). For each estuarine sample, at least three “shifted blanks” were conducted with  $t_{1,\text{sb}} = 50$  s (ESI section 2.3). The shifted blank response was subtracted from each total AGNES sample response. The residual current ( $I_\infty$ ) results from the presence of a small quantity of oxygen in the purged sample [23, 45].  $I_\infty$  was calculated as the average response current from  $t_2 = 49.55$  to 50.00 s and was subtracted from the stripping current of all samples and blanks. For AGNES measurements, the limit of detection (LOD) for each sample was calculated using  $3 \times \text{S.D.} I_{\text{sb}} / (Y\eta)$  from the corresponding shifted blanks and  $n = 4$ .

### 2.3.2 Competitive Ligand Exchange Adsorptive Cathodic Stripping Voltammetry (CLE-AdCSV)

For CLE-AdCSV a VA Computrace 797 (Metrohm) was used in conjunction with the 797 VA Computrace 1.3.2 Metrodata software for peak analysis. The Ag/AgCl reference electrode and electrolyte bridge contained 3 M KCl (Metrohm).

For the titrations, sub-samples were placed (12 x 10 mL, where one aliquot was repeated) into 30 mL plastic cups (polypropylene, Life Pharmacy) and spiked with incremental additions of Zn to a maximum concentration ca. 1.5 orders of magnitude greater than the TDZn concentration in the original sample. HEPES and APDC were

added to final concentrations of 10 mM and 40  $\mu\text{M}$ , respectively. Cups were covered and left overnight (ca. 15 h) to equilibrate.

For the quantification of  $[\text{Zn}^{2+}]$  in samples containing 250  $\mu\text{M}$  APDC, the TPM (equation 4) was used, where labile Zn was determined in two aliquots (10 mL) of buffered sample using two standard additions each. Samples and a certified reference material (CRM) were prepared for the analysis of TDZn by UV irradiation (4 h, 400 W medium pressure Hg lamp, Photochemical Reactors) of the acidified sample (ca. 30 mL) in the presence of hydrogen peroxide (final concentration 15 mM [47]). The pH was raised to ca. pH 6 using ammonia solution (SpA, ROMIL) and TDZn concentrations were determined in the same manner as labile Zn (final concentration of HEPES and APDC 10 mM and 250  $\mu\text{M}$ , respectively).

CLE-AdCSV analysis took place using differential pulse modulation in de-oxygenised (3 min purge with  $\text{N}_2$ ) samples. Deposition times of 5 – 60 s were used, depending on Zn concentration, at a potential of -0.9 V and the current response to analyte reduction (stripping was done at a potential of -1.15 V) was quantified as peak height above the baseline. Deposition times were kept to a minimum in order to avoid interference from other electroactive organic species, a problem known to affect this technique [48]. CLE-AdCSV titrations were undertaken in duplicate, one each on samples filtered to 0.4  $\mu\text{m}$  and to 0.2  $\mu\text{m}$ . The capacity (complexing capacity, CC) of Zn complexing natural ligands ( $\text{L}_x$ ) in the sample and the conditional stability constants ( $\log K$ ) of the Zn- $\text{L}_x$  complexes were calculated after data transformation according to the van den Berg/Ruzic linearization method [49]. Titrations were carried out on the 0.4 and 0.2  $\mu\text{m}$  filter fractions of each estuarine sample (Fig. 2) using 40  $\mu\text{M}$  APDC [8, 50].

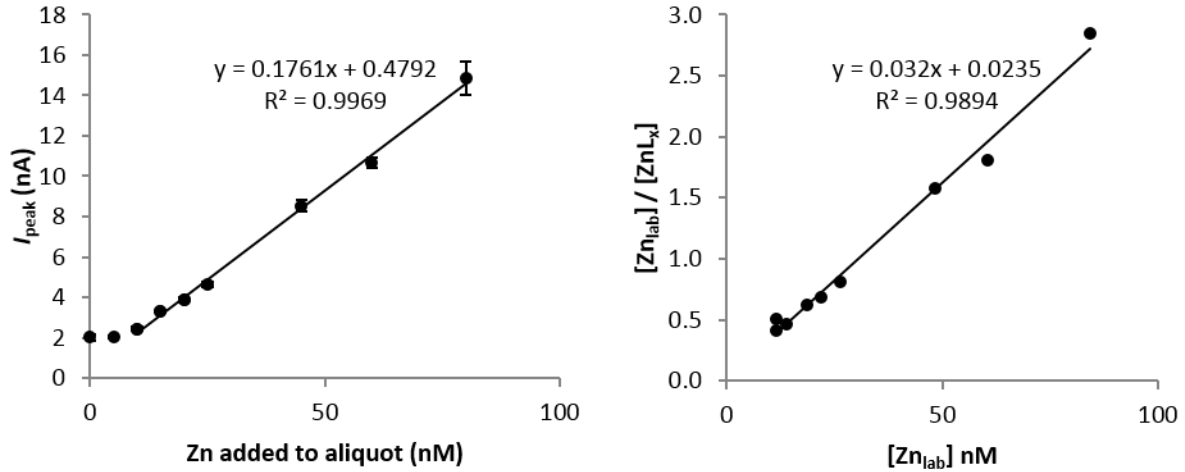


**Fig. 2** A complexation capacity titration curve (left) and transformed data (right) obtained for an estuarine sample (IS 4.8<sup>a</sup>). Error bars represent  $\pm$  95% confidence intervals ( $n = 4$ ).

Labile Zn and TDZn concentrations were also quantified in each sample (in both filtered fractions) using 250  $\mu$ M APDC as described previously. Free zinc ion concentration ( $[Zn^{2+}]$ ) was calculated via the TPM using results from CLE-AdCSV analyses with both APDC concentrations, employing equation 4 [51].

$$[Zn^{2+}] = \frac{TDZn}{(\alpha_{Zn'} + \alpha_{ZnLx})} \quad (4)$$

Where  $\alpha_{Zn'}$  and  $\alpha_{ZnLx}$  are the side reaction (alpha) coefficients [52] for complexation of  $[Zn^{2+}]$  with inorganic ligands, and natural organic ligands respectively. The former was calculated using the ion pairing model discussed previously, and the latter using Equation 5 [51]:

$$\alpha_{ZnLx} = \left( \alpha_{ZnAPDC} + \alpha_{Zn'} \right) \times \frac{(1-X)}{X} \quad (5)$$

Where  $\alpha_{ZnAPDC}$  is the alpha coefficient for the Zn-APDC complex, which equals the stability constant for Zn-APDC corrected for ionic strength ( $K'_{ZnAPDC}$ ) multiplied by the added APDC concentration, and  $X$  is the ratio of labile Zn to TDZn in the sample. Values for  $K'_{ZnAPDC}$  were calculated using constants from [19].

#### *2.3.2.1 CLE-AdCSV Analytical figures of merit*

Two replicate titrations were carried out (one each at 0.4 and 0.2  $\mu\text{m}$  filter fractions) using CLE-AdCSV with 40  $\mu\text{M}$  APDC, and two replicate aliquots of sample analysed for labile Zn and TDZn using 250  $\mu\text{M}$  APDC. During titrations, one of the aliquots was analysed three times to determine reproducibility.

For CLE-AdCSV, the LOD was calculated using 3 x S.D. of the blank ( $n = 4$ ) using a deposition time of 60 s and maximum drop size and stirring speed.

Procedural blanks for zinc were generated using UHP water, both prior to sampling and during filtration. Zinc concentrations in these blanks were analysed using CLE-AdCSV (APDC concentration = 250  $\mu\text{M}$ ).

#### *2.3.3 Dissolved Organic Carbon (DOC)*

Dissolved organic carbon was determined in acidified samples (ca. pH 2, using 6 M HCl) using high temperature catalytic combustion (Shimadzu TOC V) [53]. The instrument was calibrated at the beginning of each run and samples were sandwiched between field and UHP water blanks. Mean DOC concentrations in field procedural blanks were subtracted from each sample. A marine water CRM, (Florida Strait 700 m depth, University of Florida) was also run with each batch of samples.

#### *2.3.4 Statistical treatment of results*

Paired  $t$ -tests ( $P = 0.02$ ) were used to compare the mean  $[\text{Zn}^{2+}]$  determined using CLE-AdCSV (at both APDC concentrations) and AGNES in each sample, and  $F$ -tests were used to compare their variances [54].

For CLE-AdCSV, CRM preparation and quantification were as described for TDZn.

### **3 Results and Discussion**

### 3.1 Optimisation of the gain and deposition time

The effect of changing the gain ( $Y$ ) with its suitable deposition time ( $t_{1,a}$ ) on the response are shown in Fig. 3. From the three different deposition times applied to each sample aliquot, and the guidelines outlined in [45], it can be concluded that the longest times were sufficient to achieve equilibrium (i.e. a constant faradaic current). For the two gain settings used (e.g.  $Y = 256$  and  $514$ , Fig. 3) at the longest deposition time for each (1000 and 3000 s respectively) there was a proportional increase in the faradaic current (18.4 and 36.8 nA respectively).

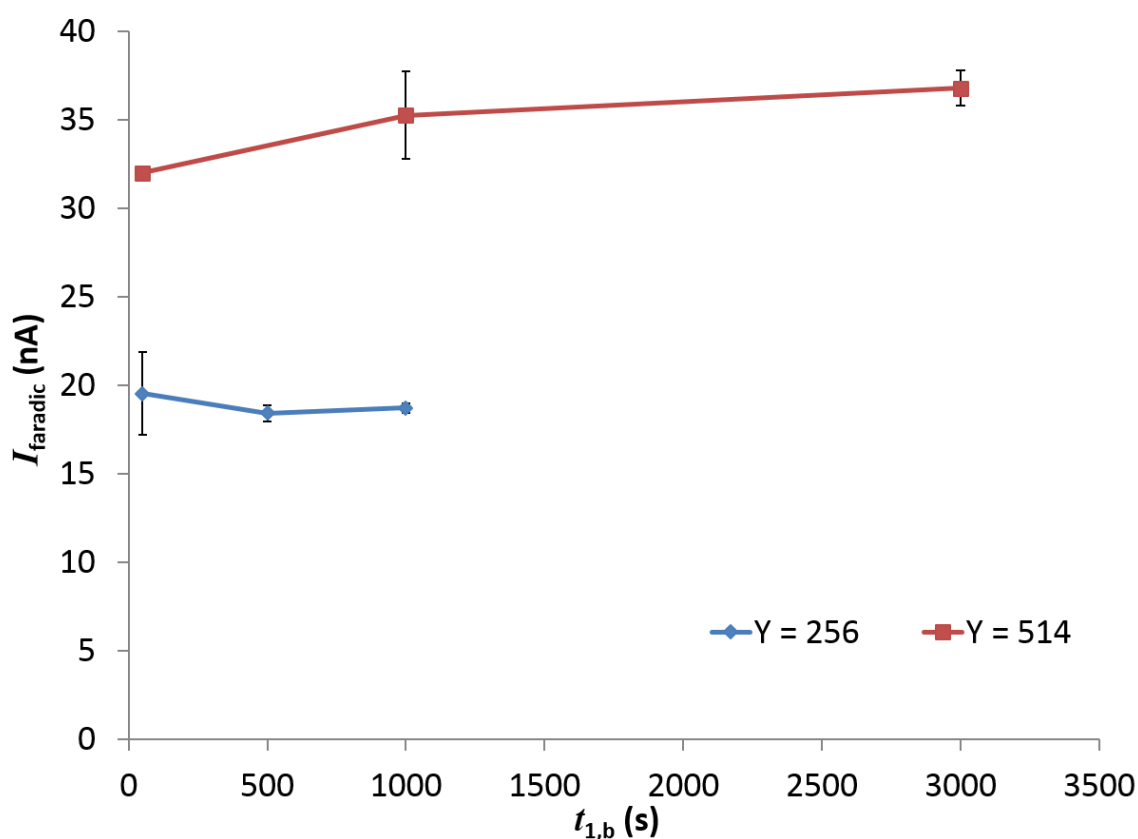


**Fig. 3** Stripping currents of AGNES measurements conducted on an estuarine sample (IS 25<sup>b</sup>) using a 2P program (ESI section 2.2) at two different gains ( $Y = 256$ ,  $t_{1,a} = 500$  s and  $Y = 514$ ,  $t_{1,a} = 1000$  s) with increasing deposition time ( $t_{1,b}$ ). Note that doubling the gain doubles the current obtained at equilibrium, indicated by the plateau reached between the second and third  $t_{1,b}$  applied, indicating consistent measurements. Error bars represent 95% confidence intervals ( $n = 4$ ).

### 3.2 Analytical figures of merit

In order to determine  $[\text{Zn}^{2+}]$  in TrAC waters it is necessary to achieve accurate measurements over the full salinity range (0 – 35) with a limit of detection (LOD) in

the low nM range. This is based on the new UK EQS of 121 nM for TDZn and the assumption, from the data in Table 1, that the  $[Zn^{2+}]$  fraction in estuarine waters is 2 - 25% of the TDZn concentration. Possible interferences from metals other than Zn present in the Tamar samples and the CRM could potentially affect the results. APDC is known to complex a number of other metals (e.g. Ca, Cd, Co, Cu, Fe, Mg, Pb) which could compete with the Zn for complexation with APDC prior to adsorption of the metal-APDC complexes on the mercury drop [48]. The fact that APDC is added in excess however, should minimise any impact on the reduction of the CLE-AdCSV signal. Intermetallic complexes formed between Cu and Zn have proved troublesome for electrochemical stripping analyses, but only at Cu concentrations in great excess of Zn [55]. Concentrations of Cu in the samples in this work were only analysed during the spring and summer surveys, but for a number of other surveys conducted on the Tamar (publication of this data in progress), Cu concentrations were repeatedly determined to be less than Zn. It is therefore unlikely that these intermetallic complexes interfered with the  $[Zn^{2+}]$  determined by the two techniques for either the samples or the CRM.

### 3.2.1 Limits of detection

AGNES calibration was performed at a similar ionic strength to that of the sample and therefore the LOD can be estimated from shifted blanks (see section 2.3.5) carried out during the calibration, the gain used for the calibration ( $Y_{\text{calibration}}$ ) and the gain used for the sample ( $Y_{\text{sample}}$ ):

$$\text{LOD of } Y_{\text{sample}} = \frac{Y_{\text{calibration}}}{Y_{\text{sample}}} \times \text{LOD of } Y_{\text{calibration}} \quad (6)$$

The LOD for AGNES is therefore implicitly related to the gain ( $Y$ ) [11, 23] and in this study ranged from 0.73 nM ( $Y = 4231$ ) to 18 nM ( $Y = 256$ ) Zn. A higher gain leads to a lower LOD, but this requires a longer deposition time to reach equilibrium, which will extend the measurement time and could result in speciation changes within the sample ([56] and references therein). In this work, analysis of a single aliquot commenced immediately after thawing a sample to room temperature and analysed within the following 48 h.



The LOD for Zn using CLE-AdCSV (3 x S.D. of the blank) is dependent on the deposition time [57] and in this work was 0.79 nM Zn with a 60 s deposition time. The procedural blanks analysed during sampling were  $\approx$  1.5 nM TDZn, which included contributions from the sample bottles, filtration units and filter membranes. This value was considered negligible for the purposes of determining  $[Zn^{2+}]$ , particularly given that the free metal ion was on average 25 % of the TDZn concentration. Procedural blank values were not subtracted from the measured concentrations because the TDZn concentration in the sample is required to accurately calculate  $[Zn^{2+}]$ .

The LOD for DOC (using 3 x S.D. of the blank) was  $10 \pm 5 \mu\text{M C}$ .

### 3.2.2 Accuracy and precision

Recoveries of  $[Zn^{2+}]$  from the Estuarine Water CRM were  $112 \pm 19 \%$  ( $n = 4$ ) for AGNES and  $103 \pm 8 \%$  for CLE-AdCSV (using 250  $\mu\text{M}$  APDC) relative to a 'derived value' of 140 nM  $[Zn^{2+}]$ . There is no commercially available CRM for free Zn ion in aqueous solutions and therefore  $[Zn^{2+}]$  at the salinity (12.1) and pH (1.5) of the irradiated CRM was predicted using thermodynamic equilibrium calculations (VMINTEQ) based on the input parameters given in ESI section 2.6.

The mean relative standard deviation (RSD) for TDZn measurements made using CLE-AdCSV was 6 %, and typical RSD for repeat aliquots analysed during titrations were  $\leq 5 \%$  ( $n = 3$ ). The mean RSD for  $[Zn^{2+}]$  determination was 18 % using AGNES and 32 % using CLE-AdCSV (two-point method). The poorer precision shown by the latter technique is attributed to the propagation of errors associated with each step required to derive a value for  $[Zn^{2+}]$  by CLE-AdCSV. The results for the DOC CRM determinations were  $47.8 \pm 0.9$ ,  $49.7 \pm 1.6$  and  $41.3 \pm 1.8 \mu\text{M C}$  ( $n \geq 3$ ) for the winter, spring and summer surveys respectively (compared with the consensus range of 41 – 44  $\mu\text{M C}$ ).

### 3.3 Comparison of AGNES and CLE-AdCSV for the determination of $[Zn^{2+}]$

Table 3 summarises the key analytical characteristics of AGNES and complexation capacity titrations (CCT) with CLE-AdCSV. They can be considered as

complementary techniques for investigating Zn speciation in TrAC waters. An attractive feature of CCT with CLE-AdCSV is that the data obtained includes free zinc ion concentrations, concentrations of (operationally defined) groups of natural ligands in the sample and their conditional stability constants with Zn. These data are necessary to reduce uncertainties associated with predictions of Zn speciation using thermodynamic equilibrium speciation codes such as Visual MINTEQ [14], but analysis does require a large sample volume (>150 mL). Furthermore, calibration by standard additions to each sample during CLE-AdCSV analysis eliminates the need for matrix matching.

The presence of surface-active organic compounds in TrAC waters can however, cause interferences through adsorption at the electrode surface during CLE-AdCSV analysis [58]. Optimisation of analytical parameters can reduce interferences, but baseline distortions and ill-defined peaks may make quantification challenging. An attractive characteristic of AGNES, shown both theoretically [23] and experimentally [26], is that the stripping signal is unaffected by such interferences, because the equilibrium value is prescribed only by the gain and  $[Zn^{2+}]$  at the electrode surface. In addition, AGNES does not generally require any additional reagents (e.g. buffers, competing ligands, metal standards) and minimal sample manipulation, thereby reducing the potential for contamination.

**Table 3** Comparison of analytical characteristics of AGNES and complexing capacity titrations (CCT) with CLE-AdCSV.

	<b>AGNES</b>	<b>CCT with CLE-AdCSV</b>
Instrumentation	Standard for voltammetry	Standard for voltammetry
Determinands	Zn <sup>2+</sup> , Pb <sup>2+</sup> , Cd <sup>2+</sup> , Cu <sup>2+</sup>	Any element forming a reducible complex with an added ligand that adsorbs on the electrode
Speciation data obtained	[Zn <sup>2+</sup> ]	[Zn <sup>2+</sup> ], complexation capacity, stability constant of complex
Salinity range	fresh to seawater	fresh to seawater
Matrix matching for calibration	Yes (calibration prior to sample analysis)	No (standard addition to each sample)
Sample volume*	10 mL	150 mL
Sample preparation time*	20 min	>15 h
Sample analysis time*	6 – 9 h	~ 1 h
Blank determination	Shifted blank	Blanks determined in UHP water (60 s deposition)
Background corrections	Shifted blank method to enable subtraction of capacitive component of analytical signal	Peak height relative to baseline; wave form parameters optimised to reduce capacitive contribution
Limit of Detection	Dependent on gain setting	Dependent on deposition time
Adsorptive interferences at electrode	No	Yes

\*Volume or time to complete analysis on one aliquot of sample at two gains and two times per gain (AGNES), or one 12-point titration with three replicate scans made on each aliquot (CLE-AdCSV).

### *3.4 Application of AGNES to TrAC waters*

TDZn concentrations in 13 estuarine samples (salinities 0.1 – 31.9), together with ancillary water quality data, are summarised in Table 4. Temperatures reflected the time of year (6.5 – 15.3 °C) and, within individual surveys, sample pH generally increased with increasing salinity. The range of observed DOC concentrations (30.9 – 482  $\mu\text{M C}$ ) and temperatures were consistent with other data reported for the Tamar [59] and other temperate estuaries [60]. DOC concentration generally decreased with increasing salinity, with the exception of one sample (IS 14<sup>b</sup>, S = 8.8, 482  $\mu\text{M C}$ , location Fig. S1). The location of this sample coincided with the onset of the high turbidity area in the narrowing upper estuary and the high DOC concentration was probably the result of tidal re-suspension of bottom sediments rich in organic matter.

**Table 4** Physico-chemical and analytical data for the estuarine samples.

Sample code*	Survey	Salinity	Ionic strength	Total dissolved Zn	[Zn <sup>2+</sup> ] ± S.D (nM) (number of replicates)		DOC (µM C)	pH	Temperature (°C)
			(M)	(nM)	AGNES <sup>†</sup>	CLE-AdCSV <sup>‡</sup>			
FW -1.1 <sup>a</sup>	Summer	0.1	0.004	126	5.7 ± 0.9 (3)	3 ± 1 (3)	245	7.79	ND
FW -1.1 <sup>b</sup>	Summer	0.1	0.004	225	7 ± 3 (7)	3 ± 1 (3)	245	7.79	ND
FW -1.1 <sup>b</sup>	Winter	0.15	0.005	129	8 ± 1 (4)	9 ± 2 (4)	114	7.19	6.0
IS 4.8 <sup>b</sup>	Winter	0.4	0.010	80	4 ± 1 (3)	2 ± 2 (4)	123	7.42	10.1
IS 13.3 <sup>b</sup>	Winter	3.8	0.075	47	11 ± 2 (4)	13 ± 2 (4)	114	7.45	7.4
IS 14 <sup>b</sup>	Spring	8.8	0.17	254	14 ± 2 (4)	46 ± 11 (4)	482	8.07	12.5
IS 19.5 <sup>b</sup>	Winter	9.5	0.18	50	12 ± 2 (3)	19 ± 4 (4)	89.3	7.83	7.3
IS 24 <sup>b</sup>	Winter	14.9	0.28	22	14 ± 2 (4)	19 ± 5 (4)	30.9	7.70	7.4
IS 19.5 <sup>b</sup>	Winter	16.2	0.30	41	23 ± 5 (4)	23 ± 5 (4)	56.2	7.86	6.8
IS 25 <sup>b</sup>	Spring	20.7	0.39	65	26 ± 4 (4)	27 ± 5 (4)	208	8.50	15.3
SW 32 <sup>b</sup>	Winter	21.1	0.39	11	2.2 ± 0.1 (4)	5 ± 4 (4)	56.5	7.80	6.5
SW 32 <sup>a</sup>	Spring	31.9	0.59	32	8 ± 1 (7)	10 ± 3 (4)	147	8.55	12.4
SW 32 <sup>b</sup>	Spring	31.9	0.59	62	5.9 ± 0.9 (8)	10 ± 3 (4)	147	8.55	12.4

\*FW Freshwater endmember; IS Intermediate salinity sample; SW Seawater endmember; numbers refer to distance (in km) from Gunnislake Weir, the tidal limit of the Tamar Estuary (note that the fresh water samples were taken upstream of the weir, hence a negative distance); <sup>a</sup>0.2 µm filter fraction; <sup>b</sup>0.4 µm filter fraction

<sup>†</sup>Represents the mean [Zn<sup>2+</sup>] for the number of replicates given in brackets.

<sup>‡</sup>Represents the mean [Zn<sup>2+</sup>] determined using 40 µM and 250 µM APDC for the number of replicates given in brackets.

TDZn concentrations were in the range 11 - 254 nM, which are in agreement with other studies on the Tamar Estuary ([61, 62]), and exceeded the current Zn EQS for saline waters (121 nM) in one sample (IS 14<sup>b</sup>). The abandoned metal mines in the Calstock/Gunnislake mining district were the main diffuse and point sources to the high TDZn concentrations observed in the freshwater end member (FWEM) and upper estuary [63].

Fig. 4 shows the  $[Zn^{2+}]$  results for AGNES and CLE-AdCSV together with the salinities for these samples, with the lowest  $[Zn^{2+}]$  concentrations ( $< 10$  nM) found in the upper and lower estuary ( $0.4 < S < 21.1$ ). In the FWEM and low salinity zone of the estuary ( $S < 1$ ), high DOC concentrations indicate the possibility of high complexing capacity for Zn that would maintain low  $[Zn^{2+}]$  ( $< 6.6$  % of TDZn). However, the discrepancy between filter pore size fractions for metals and DOC ( $0.4/0.2$   $\mu\text{m}$  and  $0.7$   $\mu\text{m}$  respectively) means that drawing a direct relationship between DOC concentrations and complexation capacity in this work is not certain. The lower TDZn concentrations due to dilution with sea water, and relatively high Zn complexation (74 – 91 %) also resulted in the low  $[Zn^{2+}]$  at the mouth of the estuary. The samples containing the highest  $[Zn^{2+}]$  (23 – 26 nM) were from the mid-estuary ( $S = 16.2 - 20.7$ ), where TDZn concentrations were moderate (41 – 65 nM), but complexation by organic ligands was relatively low (44 – 60 %). These results highlight the complexity of geochemical processes occurring in estuarine environments, where diverse fluvial and autochthonous sources of Zn and organic matter of varying complexing capacity interplay to yield a  $[Zn^{2+}]$  whose determination is an analytical challenge.

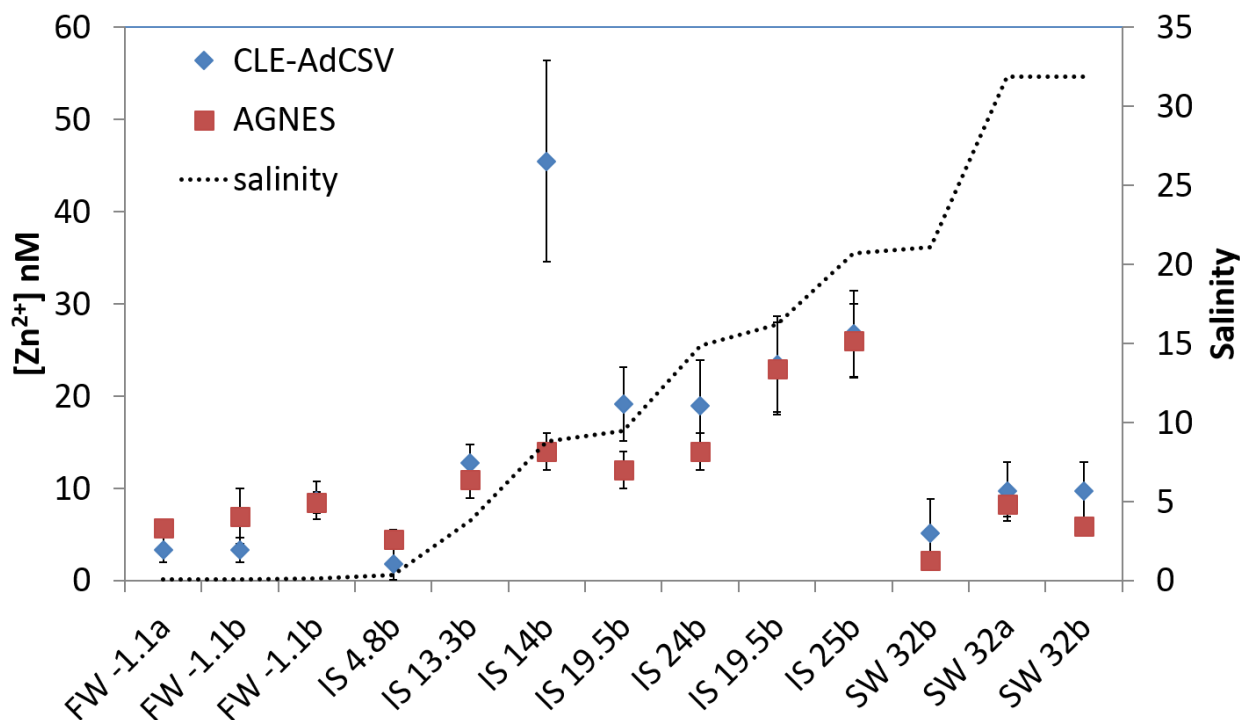


**Fig. 4** Mean  $[Zn^{2+}]$  obtained using AGNES and CLE-AdCSV and salinity for Tamar Estuary samples. Error bars represent  $\pm 1$  S.D. Note that the dotted line joining points of salinity is for illustrative purposes and does not represent a continuum

No statistically significant difference (paired  $t$ -test,  $P = 0.02$ ) was found between  $[Zn^{2+}]$  determined via AGNES (2.2 – 25 nM) and CLE-AdCSV (1.9 – 27 nM) for 12 of the samples. In sample IS 14<sup>b</sup>, however,  $[Zn^{2+}]$  determined using CLE-AdCSV was 3 fold higher than values obtained using AGNES and this sample also had a substantially higher DOC concentration (Table 4).

#### 4. Conclusions

The free zinc ion concentration ( $[Zn^{2+}]$ ) was successfully determined in thirteen estuarine samples of varying salinity (0.1 – 31.9) using Absence of Gradients and Nernstian Equilibrium Stripping (AGNES), the first time that this emerging technique has been applied to environmental samples of varying ionic strength. The benefits of AGNES, as applied to this study, include (i) a limit of detection of  $< 1$  nM  $[Zn^{2+}]$ , which is suitable for all TrAC waters, (ii) a precision of 18 % RSD over the  $[Zn^{2+}]$  range of  $\approx 2 - 26$  nM), (iii) acceptable accuracy (recovery  $112 \pm 19$  %,  $n = 3$ ) for  $[Zn^{2+}]$  and (iv) a sample processing time of ca. 2 samples per day ( $n = 4$ ). In addition, AGNES compared favourably with the

established CLE-AdCSV technique, whereby results for 12 of the 13 samples showed no significant difference ( $P = 0.02$ ) between the two methods.

Development of EQSs on the basis of bioavailable metal concentrations and predictive models is hampered by a lack of validated data for Zn speciation owing to the complex matrix and low concentrations present. Considering the practical advantages of using AGNES to determine  $[Zn^{2+}]$  in TrAC waters, and in light of the new EQS set for Zn, this technique provides the capability to advance our understanding of Zn speciation and monitor compliance with Zn EQSs.

## Acknowledgements

This PhD research is co-funded by the International Zinc Association, European Copper Institute and NERC. Warm thanks to Dr. Chris Cooper for his helpful comments, and to Marjan Heidarkhan Tehrani and Mireia Lao Martinez for their invaluable help and advice in the laboratory.

## References

- [1] S. Clemens, M.G. Palmgren, U. Krämer, *Trends in plant science*, 7 (2002) 309.
- [2] M. Pesavento, G. Alberti, R. Biesuz, *Analytica Chimica Acta*, 631 (2009) 129.
- [3] I. Johnson, WRC, 2012.
- [4] A. Stockdale, E. Tipping, S. Lofts, *Environmental Toxicology and Chemistry*, 34 (2015) 53.
- [5] L.M. Laglera, C.M.G. van den Berg, *Marine Chemistry*, 82 (2003) 71.
- [6] J.A. Nason, M.S. Sprick, D.J. Bloomquist, *Water Research*, 46 (2012) 5788.
- [7] F.L.L. Muller, S. Batchelli, *Estuarine, Coastal and Shelf Science*, 133 (2013) 137.
- [8] S.A. Skrabal, K.L. Lieseke, R.J. Kieber, *Marine Chemistry*, 100 (2006) 108.
- [9] P.B. Kozelka, K.W. Bruland, *Marine Chemistry*, 60 (1998) 267.
- [10] F.L. Muller, S.B. Gulin, Å. Kalvøy, *Marine Chemistry*, 76 (2001) 233.
- [11] J. Galceran, C. Huidobro, E. Companys, G. Alberti, *Talanta*, 71 (2007) 1795.
- [12] D.G. Heijerick, K.A.C. De Schamphelaere, C.R. Janssen, *Environmental Toxicology and Chemistry*, 21 (2002) 1309.
- [13] E. Tipping, *Computers & Geosciences*, 20 (1994) 973.
- [14] J. Gustafsson, Department of Land and Water Resources Engineering, Royal Institute of Technology, Stockholm, Sweden (2013).
- [15] S. Niyogi, C.M. Wood, *Environmental Science & Technology*, 38 (2004) 6177.
- [16] P.R. Paquin, R.C. Santore, K.B. Wu, C.D. Kavvas, D.M. Di Toro, *Environmental Science & Policy*, 3, Supplement 1 (2000) 175.
- [17] C.M.G. van den Berg, A.G.A. Merks, E.K. Duursma, *Estuarine, Coastal and Shelf Science*, 24 (1987) 785.
- [18] C.M.G. van den Berg, S. Dharmvanij, *Limnology and Oceanography*, 29 (1984) 1025.
- [19] C.M.G. van den Berg, *Marine Chemistry*, 16 (1985) 121.
- [20] I. Durán, Ó. Nieto, *Talanta*, 85 (2011) 1888.
- [21] C.M.G. van den Berg, M. Nimmo, P. Daly, D.R. Turner, *Analytica Chimica Acta*, 232 (1990) 149.
- [22] L. Gerringa, P. Herman, T. Poortvliet, *Marine Chemistry*, 48 (1995) 131.



- [23] J. Galceran, E. Companys, J. Puy, J. Cecilia, J. Garces, *Journal of Electroanalytical Chemistry*, 566 (2004) 95.
- [24] C. Parat, D. Aguilar, L. Authier, M. Potin - Gautier, E. Companys, J. Puy, J. Galceran, *Electroanalysis*, 23 (2011<sup>a</sup>) 619.
- [25] J. Galceran, D. Chito, N. Martínez-Micaelo, E. Companys, C. David, J. Puy, *Journal of Electroanalytical Chemistry*, 638 (2010) 131.
- [26] J. Galceran, M. Lao, C. David, E. Companys, C. Rey-Castro, J. Salvador, J. Puy, *Journal of Electroanalytical Chemistry*, 722 (2014) 110.
- [27] B. Pernet-Coudrier, E. Companys, J. Galceran, M. Morey, J.-M. Mouchel, J. Puy, N. Ruiz, G. Varrault, *Geochimica et Cosmochimica Acta*, 75 (2011) 4005.
- [28] C. Parat, L. Authier, A. Castetbon, D. Aguilar, E. Companys, J. Puy, J. Galceran, *Environmental Chemistry* (2014).
- [29] D. Chito, L. Weng, J. Galceran, E. Companys, J. Puy, W.H. van Riemsdijk, H.P. van Leeuwen, *Science of the Total Environment*, 421 (2012) 238.
- [30] C.A. David, J. Galceran, C. Rey-Castro, J. Puy, E. Companys, J. Salvador, J. Monné, R. Wallace, A. Vakourov, *The Journal of Physical Chemistry C*, 116 (2012) 11758.
- [31] N. Adam, C. Schmitt, J. Galceran, E. Companys, A. Vakourov, R. Wallace, D. Knapen, R. Blust, *Nanotoxicology*, 8 (2014) 709.
- [32] D. Chito, J. Galceran, E. Companys, J. Puy, *Journal of agricultural and food chemistry*, 61 (2013) 1051.
- [33] G. Alberti, R. Biesuz, C. Huidobro, E. Companys, J. Puy, J. Galceran, *Analytica Chimica Acta*, 599 (2007) 41.
- [34] J. Puy, J. Galceran, C. Huidobro, E. Companys, N. Samper, J.L. Garcés, F. Mas, *Environmental Science & Technology*, 42 (2008) 9289.
- [35] R.F. Domingos, C. Huidobro, E. Companys, J. Galceran, J. Puy, J. Pinheiro, *Journal of Electroanalytical Chemistry*, 617 (2008) 141.
- [36] M. Díaz-de-Alba, M.D. Galindo-Riaño, J.P. Pinheiro, *Environmental Chemistry*, 11 (2014) 137.
- [37] G. Benoit, S.D. Oktay-Marshall, A. Cantu, E.M. Hood, C.H. Coleman, M.O. Corapcioglu, P.H. Santschi, *Marine Chemistry*, 45 (1994) 307.
- [38] G. Wefer, F. Lamy, R. Mantoura, *Marine science frontiers for Europe*, Springer Science & Business Media, 2003.
- [39] P.W. Balls, R.E. Laslett, *Estuarine, Coastal and Shelf Science*, 33 (1991) 623.
- [40] M. Gledhill, C.M.G. van den Berg, *Marine Chemistry*, 47 (1994) 41.
- [41] D. Turner, M. Whitfield, A. Dickson, *Geochimica et Cosmochimica Acta*, 45 (1981) 855.
- [42] D. Aguilar, C. Parat, J. Galceran, E. Companys, J. Puy, L. Authier, M. Potin-Gautier, *Journal of Electroanalytical Chemistry*, 689 (2013) 276.
- [43] F. Zavarise, E. Companys, J. Galceran, G. Alberti, A. Profumo, *Analytical and bioanalytical chemistry*, 397 (2010) 389.
- [44] E. Companys, J. Puy, J. Galceran, *Environmental Chemistry*, 4 (2007) 347.
- [45] E. Companys, J. Cecilia, G. Codina, J. Puy, J. Galceran, *Journal of Electroanalytical Chemistry*, 576 (2005) 21.
- [46] P.H. Quevauviller, K.J.M. Kramer, T. Vinhas, *bcr information reference materials* (Vol. ISSN 1018 - 5593), 1993.
- [47] E.P. Achterberg, C.B. Braungardt, R.C. Sandford, P.J. Worsfold, *Analytica Chimica Acta*, 440 (2001) 27.
- [48] M. van den Berg, *Analyst*, 114 (1989) 1527.
- [49] I. Ružić, *Analytica Chimica Acta*, 140 (1982) 99.
- [50] C. M.G. Van den Berg, *Marine Chemistry*, 16 (1985) 121.
- [51] C. van den Berg, M. Nimmo, P. Daly, D. Turner, *Analytica Chimica Acta*, 232 (1990) 149.
- [52] A. Ringbom, E. Still, *Analytica Chimica Acta*, 59 (1972) 143.
- [53] E.-S.A. Badr, E.P. Achterberg, A.D. Tappin, S.J. Hill, C.B. Braungardt, *TrAC Trends in Analytical Chemistry*, 22 (2003) 819.
- [54] J.N. Miller, J.C. Miller, *Statistics and chemometrics for analytical chemistry*, Pearson Education, 2010.
- [55] D. Chito, J. Galceran, E. Companys, *Electroanalysis*, 22 (2010) 2024.
- [56] G.E. Batley, *Trace Element Speciation Analytical Methods and Problems*, CRC Press, 1989.
- [57] P.L. Croot, M. Johansson, *Electroanalysis*, 12 (2000) 565.

- [58] W. Kubiak, J. Wang, *Journal of Electroanalytical Chemistry and Interfacial Electrochemistry*, 258 (1989) 41.
- [59] A.E.J. Miller, *Estuarine, Coastal and Shelf Science*, 49 (1999) 891.
- [60] G. Abril, M. Nogueira, H. Etcheber, G. Cabeçadas, E. Lemaire, M.J. Brogueira, *Estuarine, Coastal and Shelf Science*, 54 (2002) 241.
- [61] D. Ackroyd, A. Bale, R. Howland, S. Knox, G. Millward, A. Morris, *Estuarine, Coastal and Shelf Science*, 23 (1986) 621.
- [62] K.A. Howell, E.P. Achterberg, A.D. Tappin, P.J. Worsfold, *Environmental Chemistry*, 3 (2006) 199.
- [63] K. Mighanetara, C.B. Braungardt, J.S. Rieuwerts, F. Azizi, *Journal of Geochemical Exploration*, 100 (2009) 116.

Development of Absence of Gradients and Nernstian Equilibrium Stripping (AGNES) for the determination of [Zn<sup>2+</sup>] in Estuarine Waters

Holly B.C. Pearson<sup>1</sup>, Josep Galceran<sup>2</sup>, Encarna Companys<sup>2</sup>, Charlotte Braungardt<sup>1</sup>, Paul Worsfold<sup>1</sup>, Jaume Puy<sup>2</sup>, Sean Comber<sup>1\*</sup>

<sup>1</sup> Biogeochemistry Research Centre, Plymouth University, Drake Circus, Plymouth PL4 8AA, UK.

<sup>2</sup> University of Lleida, Departament de Química, UdL and Agrotecnio. Av. Rovira Roure 191, 25198 Lleida, SPAIN.

## 1. Sampling

A map of the Tamar Estuary with sampling sites is given in **Fig. S1**.

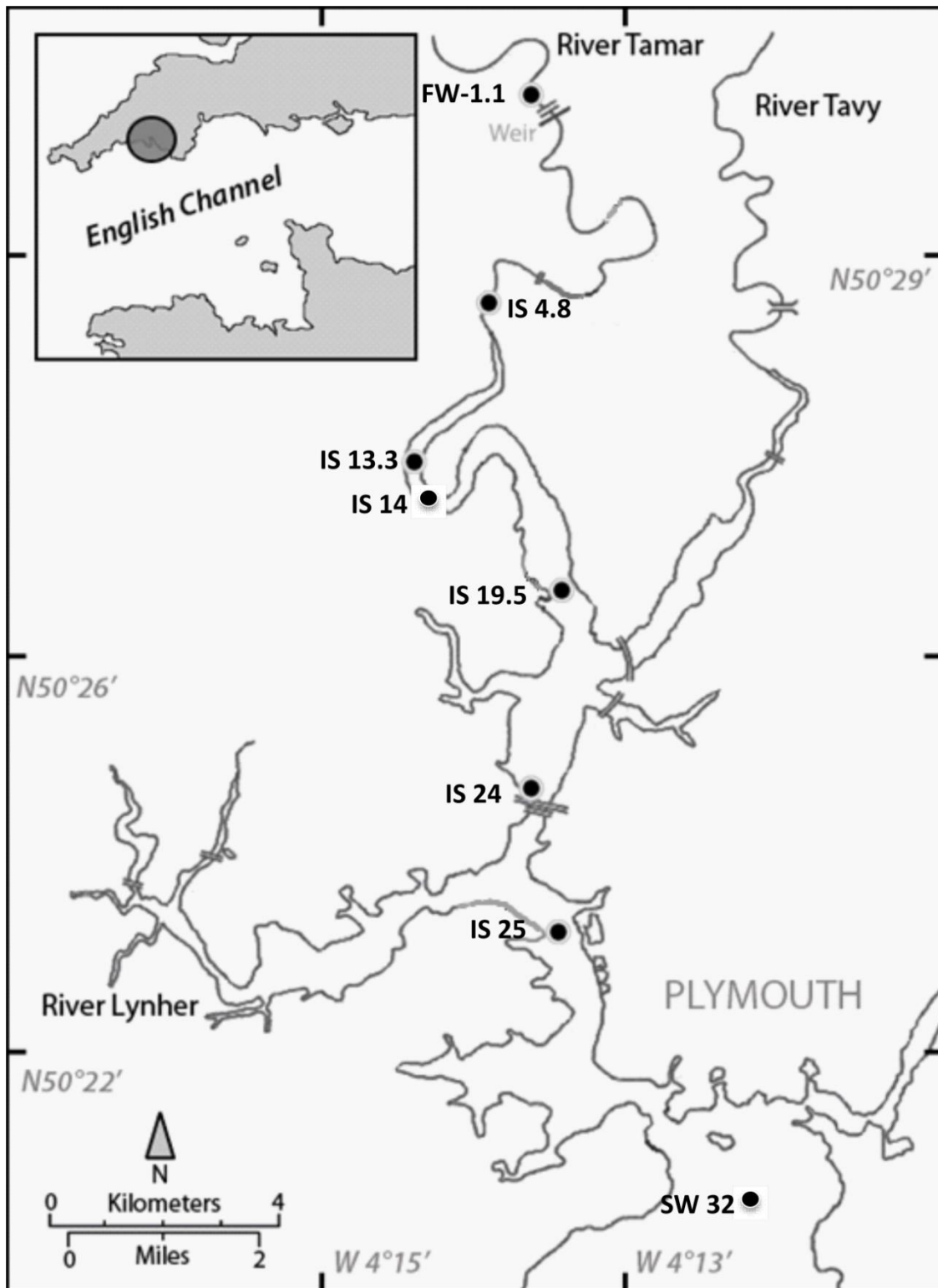


**Fig. S1** Sampling sites on the Tamar Estuary. SW: seawater end member, IS: Intermediate salinity sample, FW: fresh water endmember. Numbers refer to distance (km) from the tidal extent of the estuary, Gunnislake Weir.

## 2. AGNES Theory and Implementation

### 2.1 The AGNES 1P programme

The AGNES 1P (single potential) programme is the simplest application of AGNES, whereby the deposition stage consists of one period of deposition for a set time ( $t_1$ ) at the appropriate potential

( $E_1$ ) while the solution is stirred during  $t_1-t_w$ , followed by a quiescence period  $t_w$ . The potential is then anodically switched and a measurement is made at  $t_2$  (**Fig. S2**).

The gain and deposition time has to be carefully selected. The AGNES experiment consists of several steps:

1) The potential at the working electrode ( $E_1$ ) is applied and held constant, so that the analyte in solution is reduced and forms an amalgam with the mercury drop.

2) The concentration of the analyte within the mercury drop steadily increases with increasing time, as dictated by the presence of concentration gradients (**Fig. S3**). For instance, with a gain of  $Y = 2$ , equilibrium is achieved when the concentration of Zn within the drop is a factor of 2 greater than that in the bulk solution. A plot of  $I$  vs.  $t_1$  (**Fig. S3c**) shows a decreasing current intensity with time, until the flux of metal to the electrode ceases and current intensity remains constant.

3) A period of quiescence ( $t_w$ , **Fig. S2**) follows in order to reduce noise from stirring and to allow the mercury amalgam to stabilise.

4) A potential ( $E_2$ , more positive than  $E_1$ ) corresponding to  $Y = 10^{-8}$  is applied for time  $t_2$  (typically 50 s). This re-oxidises the analyte and strips it back into solution under diffusion limited conditions. The gradients present during this stage are illustrated in **Fig. S4a**. The oxidation current or charge ( $I$  or  $Q$ ) is measured every 0.05 s for 50 s, and its value recorded after 0.2 s (**Fig. S4b**) gives the optimum signal:noise ratio [1]. The residual current ( $I_\infty$ ) remains due to the presence of a small quantity of oxygen [1, 2], despite purging with  $N_2$  prior to analysis. This contribution of  $I_\infty$  to the desired current,  $I_{\text{faradaic}}$ , is eliminated by subtracting the average of  $I$  measured at points 49.55 to 50.00 s (**Fig. S4c**).

Except for very well-known synthetic systems, it is not possible to know the deposition time a priori. However, as a general rule of thumb for a 1P AGNES experiment with a HMDE, a safe deposition time in seconds (with stirring during  $t_1 - t_w$ , **Fig. S2**) can be set to  $7Y$ .

When the 1P programme is used for solutions with low total metal concentrations, such as relatively pristine environmental waters, the time  $t_1$  required can be prohibitively long. For such cases, the required equilibration time has been reduced with the 2P (two potential steps) AGNES programme [2].

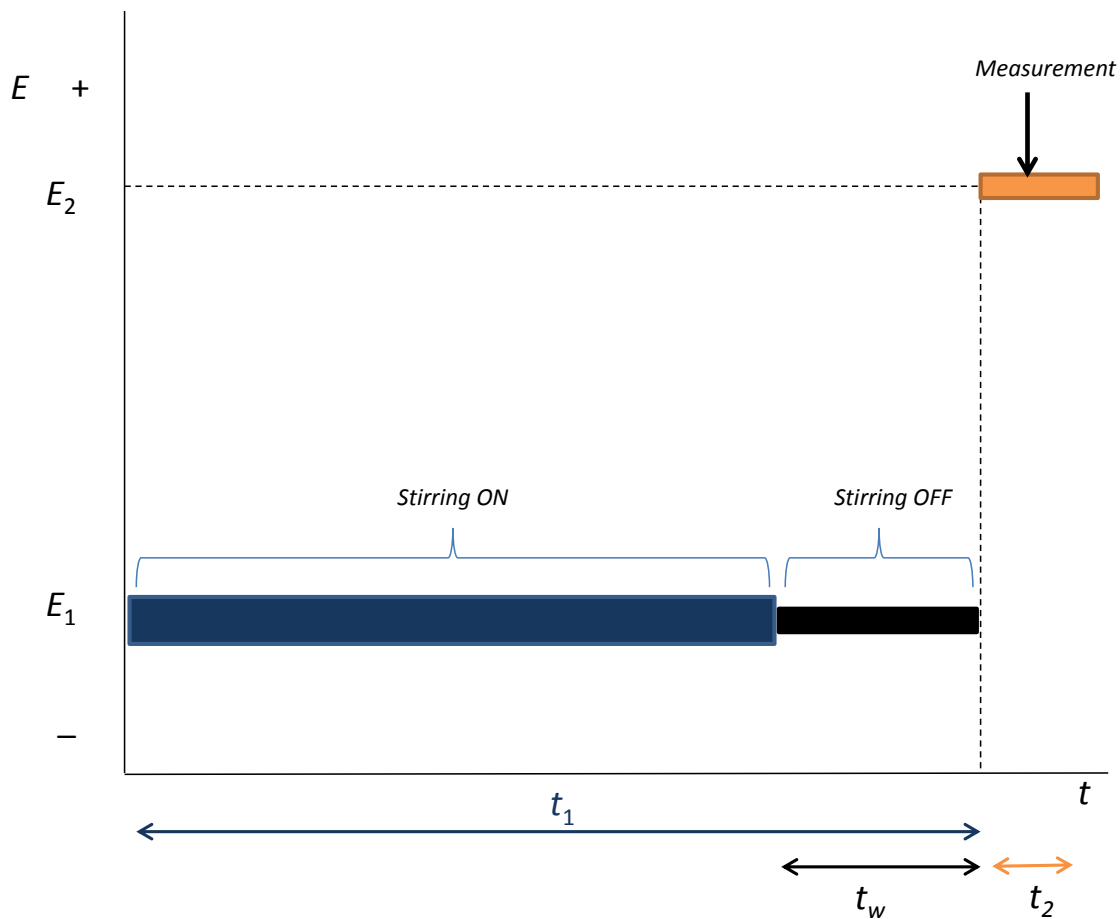


**Fig. S2** A schematic of the 1 pulse potential programme applied for an AGNES experiment. Adapted from [3].

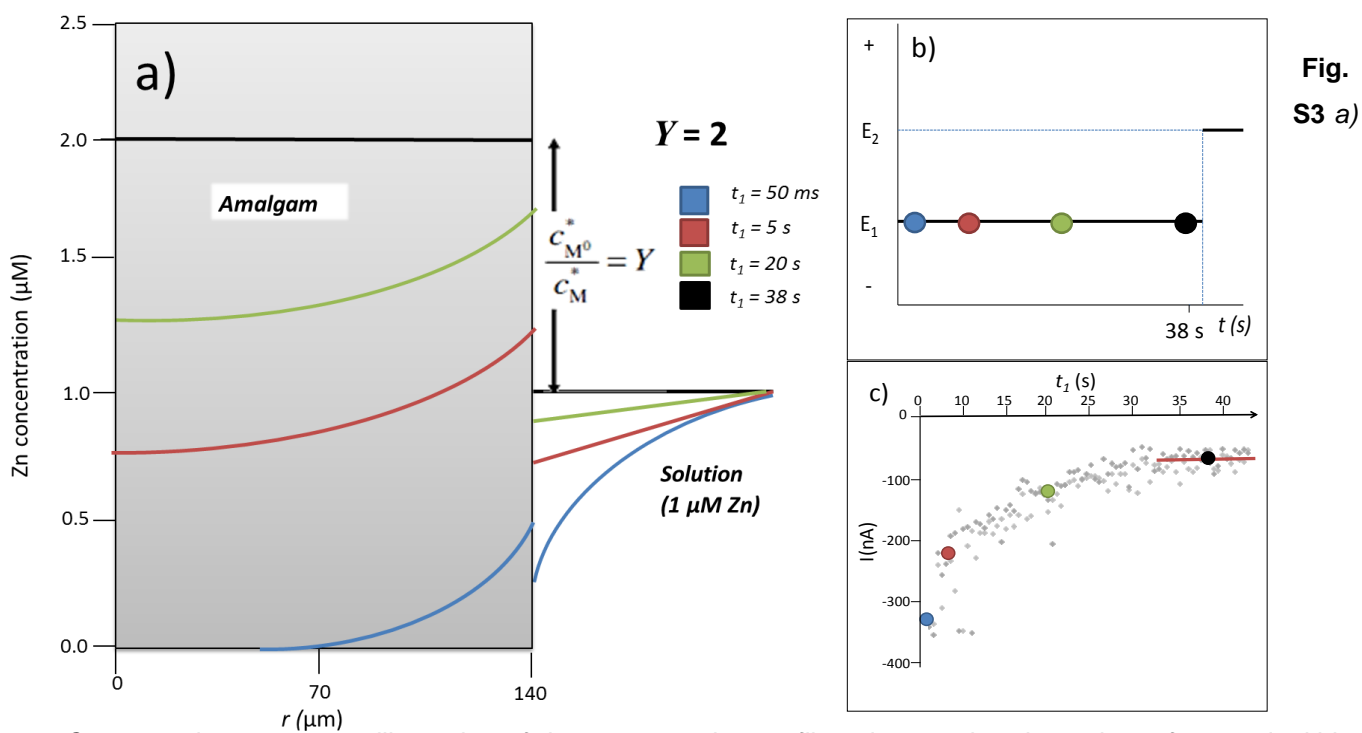


**Fig. S3 a)**

Conceptual illustration of the concentration profiles close to the electrode surface and within the mercury drop and solution with increasing deposition time  $t_1$  (represented by the different coloured lines).

The radial coordinate is denoted  $r$ , b) Schematic representation of the potential programme applied over time during deposition. The coloured dots correspond to the coloured concentration profiles in (a), c) The resulting output of (b) as a plot of current intensity vs. time. The horizontal red line highlights the plateauing of the current as equilibrium is achieved.

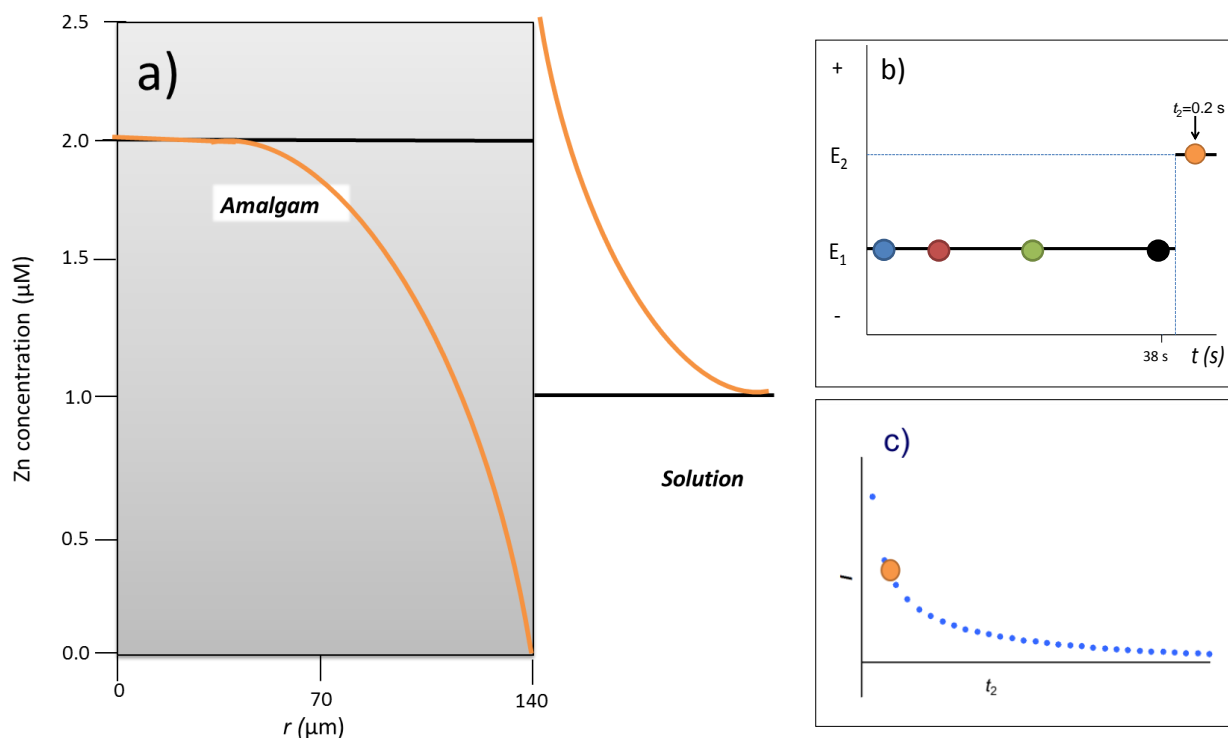


**Fig. S4**

a) The

concentration profiles (orange lines) developed within the mercury drop and solution during the stripping stage of AGNES. b) Schematic of potential over time during the deposition ( $E_1$ ) and stripping stage ( $E_2$ ).  $E_2$  is held constant for time  $t_2$  and a current measurement is recorded after 0.2 s (orange dot). c) Example of the stripping current plotted against time once  $I_\infty$  has been subtracted from each current measurement.

## 2.2 AGNES 2P programme

The two-potential-steps programme ("2P") shortens analysis time by splitting the deposition period into two sub-stages, in which two different concentration gains are applied (**Fig. S5**). The first deposition period ( $t_{1,a}$ ) occurs at a potential step corresponding to a very large gain (termed  $Y_{1,a}$ ). The potential  $E_{1,a}$ , corresponding to a practically unachievable gain (for example  $Y_{1,a} = 10^8$ ), is applied to speed up the reduction and amalgamation of the analyte, so that a high proportion of the number of moles of reduced analyte required to reach an absence of gradients enter the electrode. During a second deposition period ( $t_{1,b}$ ), the potential is stepped to  $E_{1,b}$  to implement the desired concentration gain  $Y_{1,b} = Y$ . At the end of  $t_{1,b}$ , equilibrium is achieved in the mercury drop and solution, indicated by a horizontal concentration profile (**Fig. S3a**).

If, in the application of a 2P programme, more than the desired concentration of analyte enters the mercury drop during  $t_{1,a}$ , the current at the beginning of  $t_{1,b}$  results in an *overshoot* (see Fig. 12 in [2]) of the desired constant current. Overshoot represents an excess over the desired concentration (prescribed by the actual gain), and consequently, analyte exits the mercury drop during  $t_{1,b}$  as dictated by the present concentration gradient.

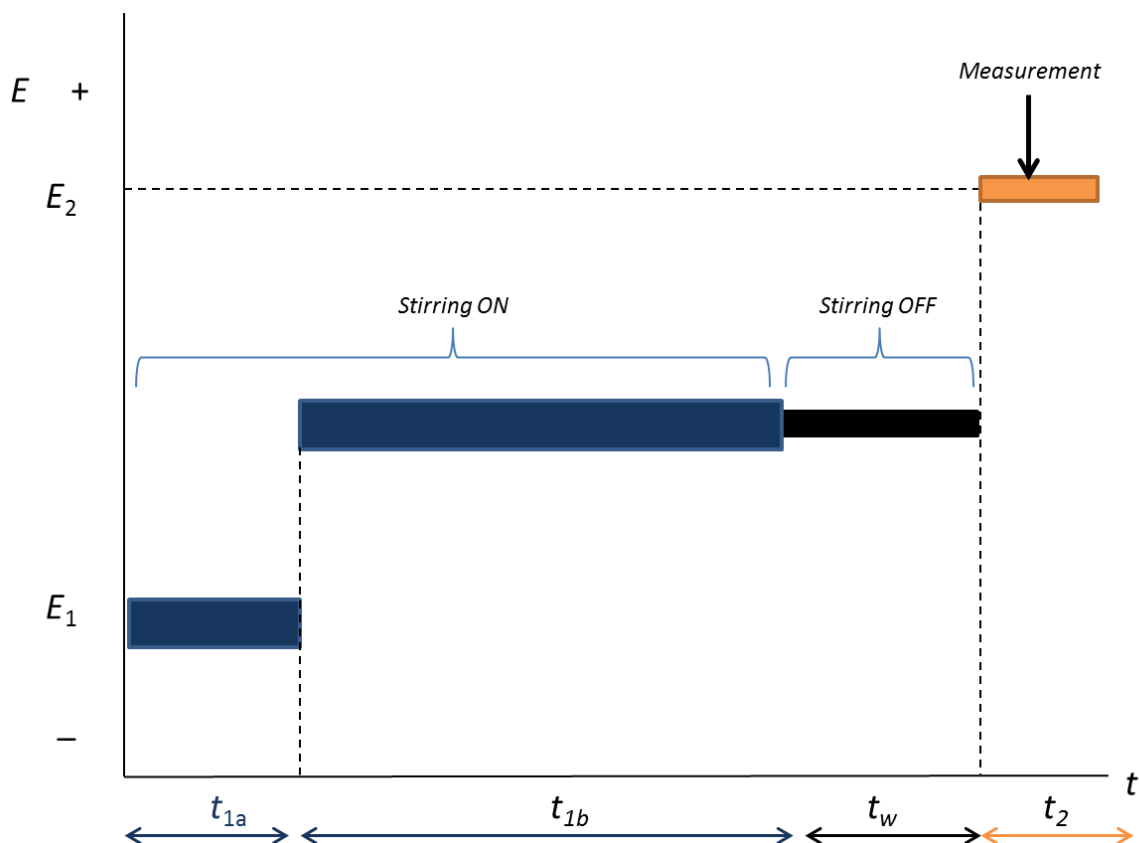


**Fig. S5** Schematic of the two-potential-steps programme applied for an AGNES experiment. Adapted from [3].

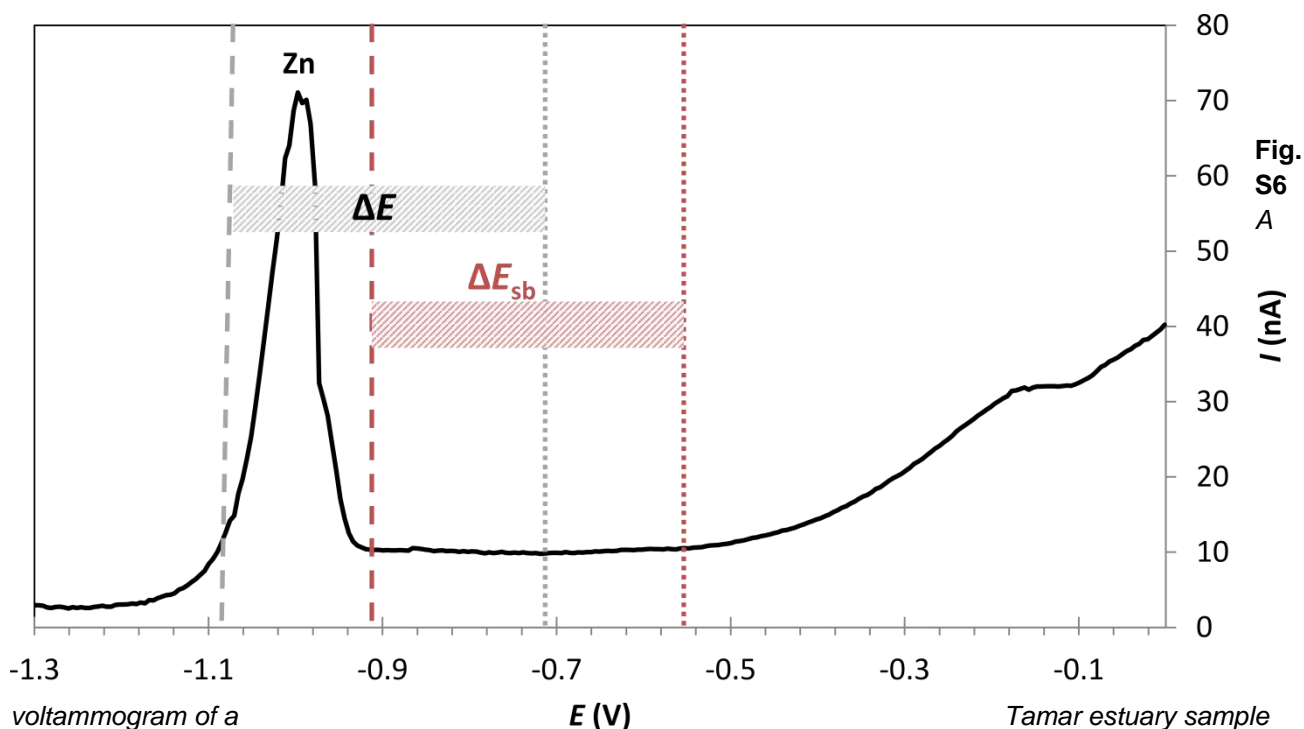
The rule of thumb for AGNES experiments with a 2P programme and HMDE,  $t_{1a} = 0.7 \times Y$  and  $t_{1b} = 3 \times t_{1a}$  [2]. This offers the operator a rough guide in optimisation of sample analysis.

### 2.3 The Shifted Blank

To illustrate how the shifted blank works, assume a solution that requires quantification of  $[\text{Zn}^{2+}]$ . A voltammogram from analysis of an estuary sample (**Fig. S6**) shows the current peaks produced after an ASV scan. So long as the potential region between the Zn and Cd peaks (ca. -0.6 V) is devoid of faradaic current produced by oxidation of Ga or Cd (red dashed area in **Fig. 6**), the “potential jump” ( $\Delta E_{\text{sb}}$ ) between a deposition potential pulse at  $E_{1,\text{sb}}$  and the potential pulse at  $E_{2,\text{sb}}$  will produce only the capacitive current ( $I_{\text{capacitative}}$ ), which can then be subtracted from the measured sample response. In the shifted blank, it is essential that the potential jump is the same in the measurement and in the blank, because the capacitive current depends on the potential change. For example, consider the AGNES potential for deposition of  $\text{Zn}^{2+}$ ,  $E_1$ , to correspond to a  $Y$  of 500 (“ $Y_1$ ”) and the stripping potential,  $E_2$ , to correspond to a  $Y$  of  $10^{-8}$  (“ $Y_2$ ”).  $E_{1,\text{sb}}$  will correspond to a negligible gain (such as 0.01, “ $Y_{1,\text{sb}}$ ”), and the stripping potential will correspond to  $Y_{1,\text{sb}} \times Y_2 / Y_1$  so that  $E_2 - E_1 = E_{2,\text{sb}} - E_{1,\text{sb}}$  (**Fig. S6**).



A check was made to ensure faradaic current from Ga or Cd was not contributing to the capacitive signal by incrementally increasing the deposition time ( $t_{1, sb}$ ) of the shifted blank on an estuary sample (Fig. S7). Results illustrate a negligible current increase after 50 s deposition.



voltammogram of a Tamar estuary sample (salinity = 17) using ASV (deposition time = 1000 s), showing current peaks and the AGNES potentials used to perform the shifted blank ( $t_{1, sb} = 1000$  s). The grey dashed ( $E_1$  corresponding to  $Y = 5000$ ), and dotted ( $E_2$  corresponding to  $Y_2 = 10^{-8}$ ) vertical lines represent potentials of AGNES measurements. The red dashed ( $E_{1, sb}$ , for  $Y_{1, sb} = 0.01$ ) and dotted ( $E_{2, sb}$ , for  $Y = 0.01 \times Y_2 / Y_1$ ) vertical lines represent potentials used for the shifted blank in order to quantify capacitive current. The difference in the potential ("jump") from  $E_1$  to  $E_2$  ( $\Delta E$ ), and  $E_{1, sb}$  to  $E_{2, sb}$  ( $\Delta E_{sb}$ ) is equal.

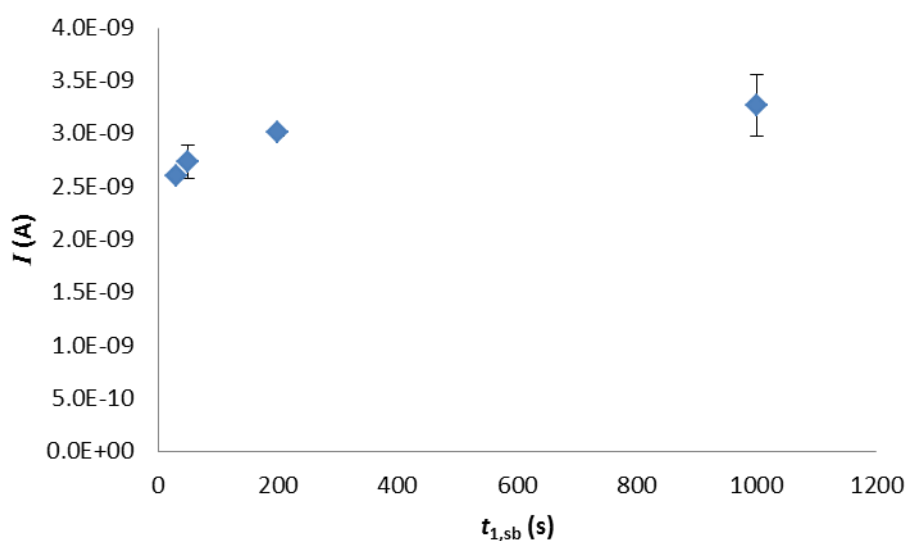


Fig. S7 Increasing the deposition time of the shifted blank ( $t_{1, sb}$ ) to check for possible contribution from Cd or Ga. Diamonds represent the average of two repeat AGNES analyses at each  $t_{1, sb}$  with error bars representing the range.

## 2.4 Obtaining the potentials for applying gain Y

The relationship between a specific potential ( $E_1$ ) and the corresponding gain Y can be derived from Nernst equation:

$$Y = \frac{[Zn^0]}{[Zn^{2+}]} = \frac{\gamma_{Zn^{2+}}}{\gamma_{Zn^0}} \exp \left[ \frac{nF}{RT} (E_1 - E^0) \right] = \exp \left[ \frac{nF}{RT} (E_1 - E^{0'}) \right] \quad (1)$$

Where  $Zn^0$  is Zn in its reduced form inside the mercury electrode

$Zn^{2+}$  represents free ionic Zn in the bulk solution (and at the electrode surface)

$\gamma_i$  is the activity coefficient of species  $i$  (computed with Davies equation)

$E_1$  is the potential of the working electrode during deposition

$E^0$  is the standard redox potential

$E^{0'}$  is the formal standard potential

$F$  the faraday constant

$R$  the gas constant

$T$  temperature

The peak potential ( $E_{peak}$ ) for Zn in a DPP experiment (**Fig. S8**), obtained after the highest Zn addition during calibration, can be used to compute gain Y through:

$$Y = \sqrt{\frac{D_{Zn}}{D_{Zn^0}}} \exp \left[ -\frac{nF}{RT} \left( E_1 - E_{peak} - \frac{\Delta E}{2} \right) \right] \quad (2)$$

Where  $\Delta E$  is the modulation amplitude of the experiment

$D_{Zn}$  and  $D_{Zn^0}$  are the diffusion coefficients for the free Zn ion and reduced Zn (inside the amalgam), respectively

The parameters for the DPP experiment used are given in **Table S1**.

**Table S1** Parameters used for attainment of a zinc DPP  $E_{peak}$

Parameter	Value
Initial scanning potential	-0.85 V
Final scanning potential	-1.05 V
Step potential	0.00105 V
Amplitude	0.04995 V
Modulation time	0.05 s
Interval time	1 s
Drop size	3 (max.)
Stirrer setting	6 (max.)

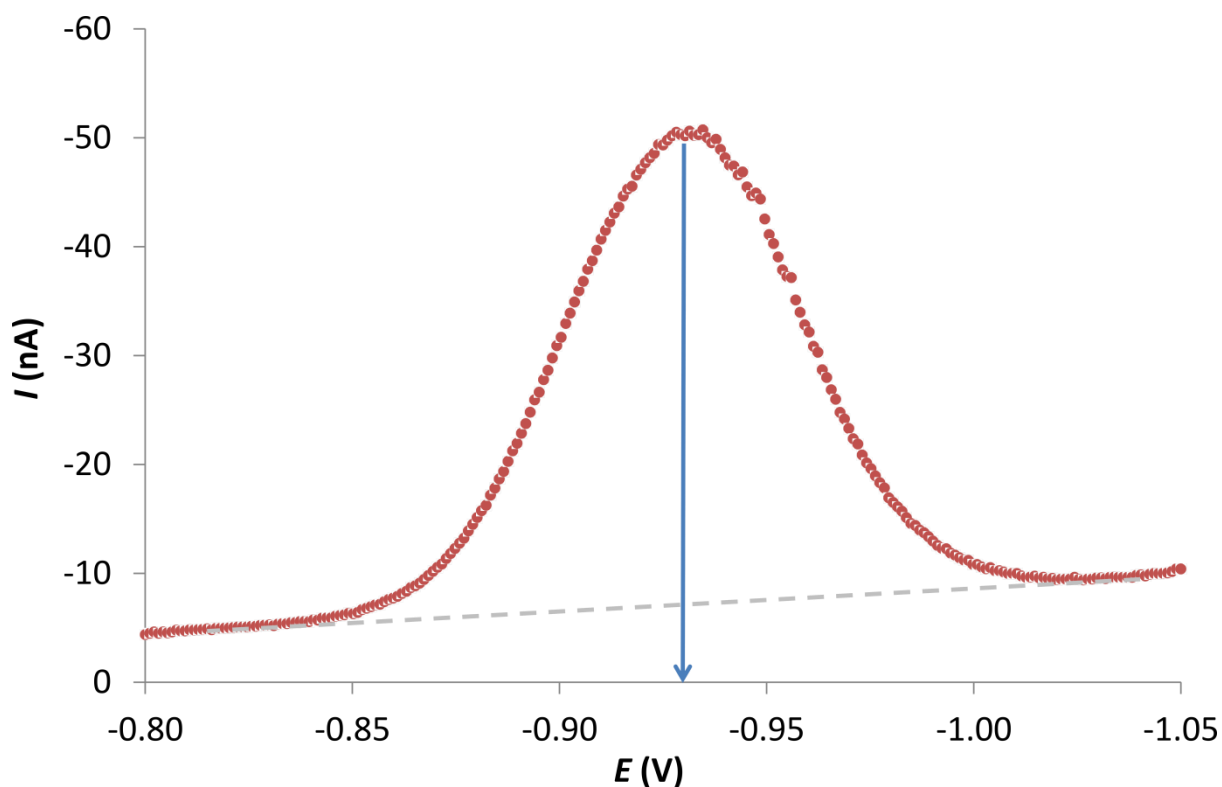


**Fig. S8** A DPP peak obtained for zinc by application of the parameters given in **Table S1** ( $\text{KNO}_3 = 0.393 \text{ M}$ , total dissolved Zn =  $10.6 \mu\text{M}$ ,  $\text{pH} = 3.45$ ). The  $E_{\text{peak}}$  is marked by the blue arrow.

## 2.5 AGNES Calibration

The slope of the calibration plot when the faradaic current ( $I_f$ ) (or the charge, Q) is plotted against Y times  $[\text{Zn}^{2+}]$ , corresponds to the proportionality factor eta ( $\eta$ , or  $\eta_Q$  when charge is used).

The input parameters for the calculation of  $[\text{Zn}^{2+}]$  and  $\{\text{Zn}^{2+}\}$  using VMINTEQ for the calibration plot shown in **Fig. 1** in the manuscript are given in **Table S2**. The  $\{\text{Zn}^{2+}\}$  output value for the given example was  $2.39 \times 10^{-6}$ . This value was calculated using VMINTEQ from the final calibration point, and was used to recalculate the actual applied Y to the sample in each case.

**Table S2** Visual MINTEQ input parameters and output values for the AGNES calibration shown in **Fig. 1** in the manuscript (solution D,  $[\text{KNO}_3] = 0.393 \text{ M}$ ). Temperature was set to ambient room temperature ( $22.5 \text{ }^\circ\text{C}$ ) and ionic strength left "to be computed". All concentrations are in M.

Input				Output
pH (fixed)	$\text{K}^+$	$\text{NO}_3^-$	Zn added	$[\text{Zn}^{2+}]$
3.700	0.39132	0.39162	$1.9796 \times 10^{-6}$	$1.61 \times 10^{-6}$
3.640	0.39081	0.39112	$3.9540 \times 10^{-6}$	$3.22 \times 10^{-6}$

3.540	0.39004	0.39035	$6.9817 \times 10^{-6}$	$5.68 \times 10^{-6}$
3.450	0.38911	0.38943	$1.0599 \times 10^{-5}$	$8.63 \times 10^{-6}$

## 2.6 CRM for AGNES

The input parameters for deriving, with VMINTEQ, the  $[Zn^{2+}]$  in the estuarine CRM BCR-505 (European Commission) is given in **Table S3**. The major ion concentrations were calculated using the ion pairing model described in **section 2.3.1** of the main article. The output VMINTEQ  $[Zn^{2+}]$  was  $1.4 \times 10^{-7}$  M.

**Table S3** Visual MINTEQ input parameters for the derivation of  $[Zn^{2+}]$  in the estuarine certified reference material BCR-505. Temperature was fixed at 22.5 °C, pH at 1.5, and ionic strength was set to “to be calculated”.

Species	Input total concentration (M)
Zn <sup>2+</sup>	$1.72 \times 10^{-7}$
K <sup>+</sup>	$3.58 \times 10^{-3}$
Na <sup>+</sup>	$1.62 \times 10^{-1}$
Mg <sup>2+</sup>	$1.85 \times 10^{-2}$
Ca <sup>2+</sup>	$3.83 \times 10^{-3}$
Sr <sup>2+</sup>	$3.18 \times 10^{-5}$
Cl <sup>-</sup>	$1.89 \times 10^{-1}$
Br <sup>-</sup>	$2.91 \times 10^{-4}$
SO <sub>4</sub> <sup>2-</sup>	$9.87 \times 10^{-4}$
F <sup>-</sup>	$2.7 \times 10^{-5}$

## 3. Complexation capacity titrations with Adsorptive Cathodic Stripping Voltammetry

This technique determines the complexation capacity (CC) and mean affinity ( $\log K$ ) of the dissolved organic matter for zinc, and the free metal ion concentration  $[M^{n+}]$  in a sample, by setting up a competitive equilibrium with the natural sample ligands ( $L_x$ ) and an added artificial ligand (AL). A small proportion of the complexes of the target metal (M) with the AL form a monomolecular layer on the surface of a hanging mercury drop working electrode during deposition at a specific oxidising potential applied for a fixed time. The potential is then swept in the cathodic direction and the complexes are reduced and stripped from the electrode surface, producing a current proportional to the labile metal concentration in solution. The determined labile concentration is operationally defined by the degree of competition between AL and  $L_x$  for complexing metal (M),

which is governed by the AL concentration added. Thus, the AL concentration used governs the “detection window” (DW) of the method, within which the CC, log K and  $[M^{n+}]$  may be determined. The lower limit of the DW is determined by the sensitivity of the technique, and the upper limit technique precision [4]. The centre of the DW equals the alpha coefficient for the formation of the MAL complex ( $\alpha_{MAL}$ ), with values for  $\alpha_{MLx}$  within approximately one decade either side being measurable [5].

For CC titrations, the sample is separated into several aliquots (ca. 10 - 12) which are spiked with incrementally increasing additions of (zinc) metal, a pH buffer (HEPES, pH 7.8) and the AL (in this case ammonium pyrrolidine dithiocarbamate, APDC). Complexation of the additional zinc by sample ligands is shown as a curve on a plot of current vs. added analyte concentration (Fig. 2 in manuscript). Transformation of these data (in this case, the van den Berg/Rusic plot [6, 7]) gives the labile Zn ( $Zn_{lab}$ ) concentration that is defined as the concentration of  $Zn^{2+}$  plus natural ligand complexes from which Zn will dissociate during the timescale of the analysis to form ZnAPDC complexes and is calculated as  $i_p$  divided by the slope of the linear portion of the titration plot (Fig 2 in manuscript). The  $ZnL_x$  concentration is equal to TDZn in the aliquot (initial TDZn concentration + spiked Zn concentration) minus  $Zn_{lab}$ . A plot of  $Zn_{lab}/ZnL_x$  vs.  $Zn_{lab}$  gives a straight line in the case of one ligand class present. Sample CC can be calculated as the inverse of the slope of the transformed plot. The log K of the  $ZnL_x$  complex is calculated from:

$$\text{Log } KZnL_x = \log (\alpha' / (\text{CC} \times \text{intercept})) \quad (3)$$

Where  $\alpha'$  is the overall alpha coefficient ( $\alpha_{Zn} + \alpha_{ZnAPDC}$ ) and ‘intercept’ is the intercept of the transformed plot (right hand plot in Fig. 2 of the paper).

## 4. References

- Galceran, J., et al., *AGNES: a new electroanalytical technique for measuring free metal ion concentration*. Journal of Electroanalytical Chemistry, 2004. **566**(1): p. 95-109.
- Comanys, E., et al., *Determination of  $Zn^{2+}$  concentration with AGNES using different strategies to reduce the deposition time*. Journal of Electroanalytical Chemistry, 2005. **576**(1): p. 21-32.
- Galceran, J., et al., *AGNES: a technique for determining the concentration of free metal ions. The case of Zn (II) in coastal Mediterranean seawater*. Talanta, 2007. **71**(4): p. 1795-1803.
- Town, R.M. and M. Filella, *A comprehensive systematic compilation of complexation parameters reported for trace metals in natural waters*. Aquatic sciences, 2000. **62**(3): p. 252-295.
- van den Berg, C.M.G. and J.R. Donat, *Determination and data evaluation of copper complexation by organic ligands in sea water using cathodic stripping voltammetry at varying detection windows*. Analytica Chimica Acta, 1992. **257**(2): p. 281-291.
- Van Den Berg, C.M.G., *Determination of copper complexation with natural organic ligands in seawater by equilibration with  $MnO_2$  I. Theory*. Marine Chemistry, 1982. **11**(4): p. 307-322.
- Ružić, I., *Theoretical aspects of the direct titration of natural waters and its information yield for trace metal speciation*. Analytica Chimica Acta, 1982. **140**(1): p. 99-113.

